Title	ステロイド側鎖を含むラビングしたポリイミド膜の光第二高調波発生
Author(s)	Ullah, Muhammad Samir
Citation	
Issue Date	2017-03
Type	Thesis or Dissertation
Text version	ETD
URL	http://hdl.handle.net/10119/14254
Rights	
Description	Supervisor:水谷　五郎，マテリアルサイエンス研究科，博士

Optical Second Harmonic Generation From Rubbed Polyimide Containing Steroidal Structure Side Chains

MUHAMMAD SAMIR ULLAH

Japan Advanced Institute of Science and Technology (JAIST)

Doctoral Dissertation

Optical Second Harmonic Generation From Rubbed Polyimide Containing Steroidal Structure Side Chains

MUHAMMAD SAMIR ULLAH

Supervisor:

Professor Dr. Goro Mizutani

School of Materials Science, JAIST

Japan Advanced Institute of Science and Technology (JAIST)

March 2017

CONTENTS

Dedicated to

My parents & wife

Sabirah & Sadid

Acknowledgement

All the admiration to the almighty Allah, the most merciful, has enabled me to do this research work.

It is a great pleasure to express my deepest sense of gratitude and sincere appreciation to my supervisor, **Professor Goro Mizutani,** School of Materials Science, Japan Advanced Institute of Science and Technology (JAIST) for his scholastic supervision, discussion and constructive guidance throughout the progress of this research work.

I would like to express my pleasure thanks to JSR Corporation Ltd., Mie 510-8552, Japan for giving the opportunity to study and research work on the polymer thin film. I would also like to a very special thank to Professor Hiroshi Mizuta and Hidekazu Tsutsui, Associate Professor, School of Materials Science, Japan Advanced Institute of Science and Technology (JAIST) for their help during this research work.

I would like to a very special thanks to Khuat Thi Thu Hien, Assistant Professor School of Materials Science, Japan Advanced Institute of Science and Technology (JAIST) for her cooperation and help during this research work. I would also like to a very special thanks to Shohei Asai, M-2 student, School of Materials Science, Japan Advanced Institute of Science and Technology (JAIST) for his cooperation and help during this research work.

I would like to thanks for the moral support and inspiration from my wife Nasrin Parvin during this research work.

Abstract

I have studied the optical second harmonic generation (SHG) of a rubbed novel polyimide (PI) film having steroidal structure side chains prepared by spin coating on an indium tin oxide (ITO)-coated glass substrate. In this measurement, for the excitation light of SHG, I used the second harmonic light of Nd: YAG laser with wavelength of 532 nm , a pulse duration of 30 ps and a repetition rate of 10 Hz. The SHG intensity as a function of the rotational angle ψ of the rubbed and unrubbed PI thin films with steroidal structure side chains diamine A with input/output polarization combinations are observed. ψ is defined as zero degree when the wave vector component of the incident beam parallel to the film face is in the same to the rubbing direction. The signal of SHG from the unrubbed PI films is isotropic in the rotational angle. There was no anisotropy in the SHG patterns from the unrubbed polymer film. The characteristic anisotropic patterns are observed due to the rubbing for all the polarization combinations. By the rubbing treatment, the side chains are thought to be pulled on the surface by the nylon cloth and the main zigzag chains lying perpendicular to the rubbing direction are pulled in the rubbing direction. The second order nonlinear susceptibility $\chi_{ijk}^{(2)}$ elements were obtained from the fitting of the SHG intensity patterns. The symmetry of the polymer chains is *Cs* symmetry with the rubbing direction parallel to the mirror plane. The average polar (tilt) angle of the rubbed PI chains was determined to be around 16^{o} by using the measured $\chi_{ijk}^{(2)}$ elements in the complex plane.

Keywords: Second harmonic generation, Liquid crystal displays, Polyimide, Rubbing treatment, Steroidal structure.

List of Figures

Chapter 1

Chapter 2

Chapter 3

Chapter 4

Chapter 5

List of Tables

Chapter 1

General Introduction

1.1 Brief review of the liquid crystal

Liquid Crystal materials are wonderful materials having interesting physical, optical and electrical properties. Liquid crystal (LC) has a stable phase and it is characterized by anisotropic properties without the existence of a three dimensional crystal lattice, generally lying between the solid crystals and conventional liquid [1]. The distinguishing characteristic of the liquid crystalline state is the pointing vector, which define the tendency of the molecules to point along a common axis. This is in contrast with the molecules of the liquid phase, which have no intrinsic order. The characteristic orientational order of the liquid crystal state is between the traditional solid and liquid phases and this is the origin of the term mesogenic state, used synonymously with liquid crystal state. The orientations of the molecules are shown in figure 1.1. Anisotropic substances may have several liquid crystal phases as shown in figure 1.2.

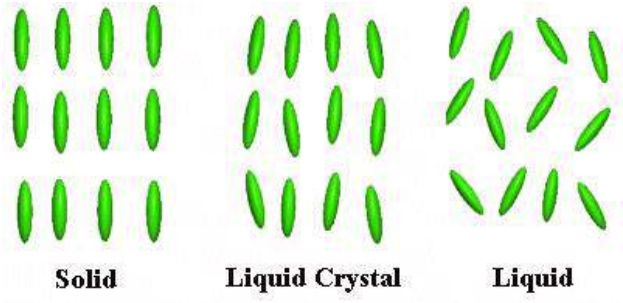

Fig.1.1 Molecular order of the liquid crystal

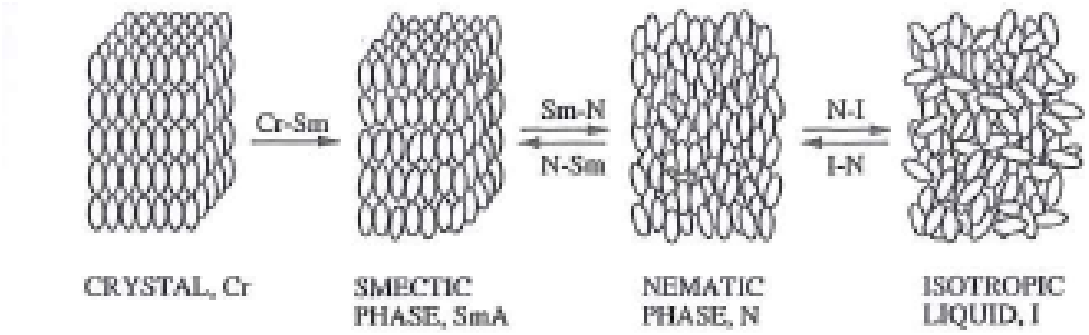

Fig.1.2 Liquid Crystal Phases [1]

The nematic LC phase is technologically important due to its fast response time. The nematic phase is defined by long range orientational order, in particular, molecules tend to align along the preferred direction. Smectic-A type: molecular alignment is perpendicular to the layer surface, but it lacks order within each layer. Smectic-C type: molecules have a tilted angle with the layer surface normal. Smectic-B type: molecular alignment is perpendicular to the layer surface and well ordered within each layer. These LC states are shown in figure 1.3.

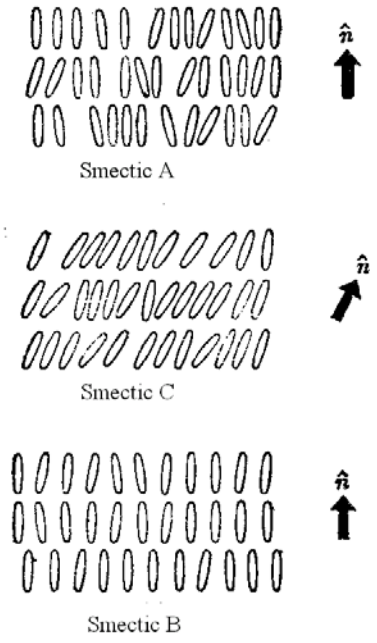

Fig.1.3 Different types of the Smectic [1]

1.2 Flat panel display and the role of LC molecule

Recently, liquid crystal displays (LCDs) are largely used in mobile phones, computers and television, because they offer a unique combination of low cost and low power consumption [2]. An alignment film material is necessary for doing the improvement of the display performance of LCD panels such as high contrast, high response time, and wider viewer angle. Liquid crystal displays (LCDs) are quite widely used in home electric appliances, industry equipment's and other devices having displays [3]. In LCDs, the orientation of liquid crystal molecules on the alignment polymer film substrates is regulated by the applied voltage in the devices. These alignment polymer films directly affect on the orientation of the liquid crystal molecules and are indispensable components in forming the LCDs.

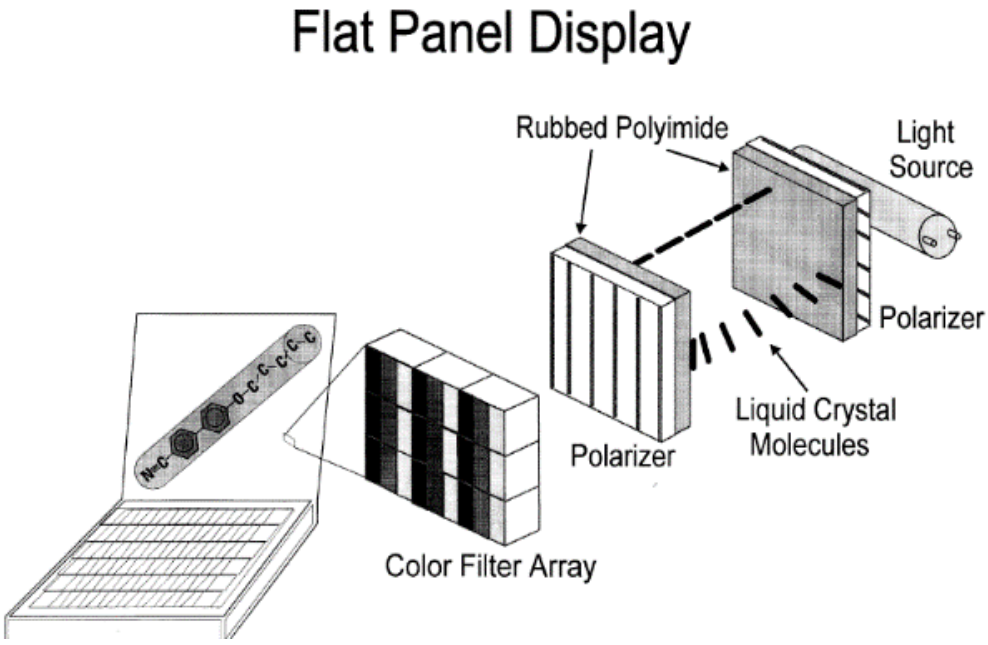

Fig. 1.4 Laptop computer flat panel display [4]

Now-a-days, laptop computers use flat panel displays due to the advantages of their light weight and smaller size. The picture is composed of many pixels on the screen. Each pixel is created by different colour of different intensities i.e. patterned color filter array as shown in figure 1.4. The intensity of the color is controlled with the help of liquid crystals to change the light intensity from the back to the front of the display. Since, the LC consists of rod like molecules which can turn to align themselves so that the long directions of the rods are parallel. In order to understand how the display work, let's consider that LC is filled into gap between two polyimide films coated onto indium tin oxide(ITO) electrode. Therefore, LC molecules can turn onto two glass plate cross polarizers. LC molecules have to be anchored down nearly parallel to the surfaces of the polyimide film such that they form a twisted helix from

(a) (b)

(c)

Fig.1.5 Application of LCD device

one side to another. When the light is coming from the back of the first polarizer, it is polarized along the long axis of the LC molecules. Then the light progresses through the helical LC structure, and changes the polarization of the light from linear to elliptical. Finally light is transmitted by the second polarizer. When the voltage increases , the LC long axis becomes parallel to the electric field direction. Thus the orientational changes in LC alignment are the main key factor for the LCD device.

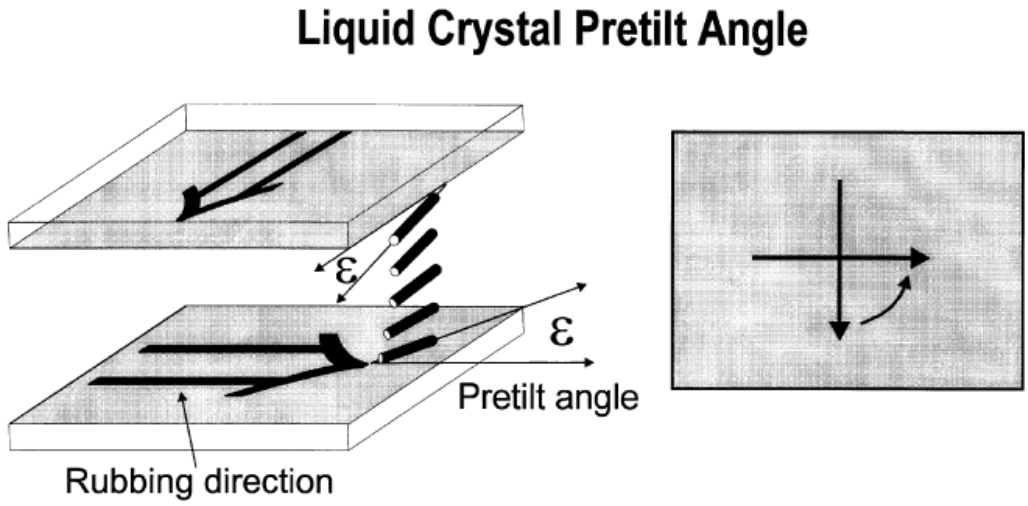

Fig.1.6 LC Pretilt angle [4]

When a nematic liquid crystal consists of rod like molecules, it is placed on a rubbed polymer surface. It exhibits both in plane and out of plane orientation of the rods. The in plane alignment direction of the rods coincides with the rubbing direction. The average upward tilt angle of the rods from the polymer surface plane, which is called as the pretilt angle, is shown in figure 1.6. The pretilt angle depends on the monomer structure of the polyimide i.e. it varies with the main chain as well as side

chain structure. It also depends on the structure of the LC molecule. The pretilt angle is technologically important, for example, it needs to exceed about 3^{o} for proper function of the display. If the pretilt angle becomes zero, there exists an ambiguity in the twisting of the LC helix between two anchored, orthogonal ends. From that point of view, it is necessary to control the pretilt angle of the LC molecule for developing the performance of the flat pannel display.

1.3 Review of Polyimide

The term polymer is derived from the Greek words ‘poly’, which means many, and ‘mer’, which means part. A polymer is, in general, a soft matter consisting of a long chain molecule, known as a macromolecule. This macromolecule is composed of a large number of repeating units, called ‘monomer’ [5]. Now-a-days different types of polymers are progressively being used in modern technology to replace conventional engineering materials like metal, steel, rock, alloys, wood and so on [6]. In addition, polymer materials are broadly used in our social life as well as in our modern science and technology, for instance, household appliances, textiles, insulation materials, medical implants, materials for optoelectronics [7]. On the other hand, the synthetic polymers can be produced inexpensively, and their properties may be managed to a degree so that many of them are superior to their traditional engineering and natural counterparts. For instance, metal and wood are replaced in some applications by synthetic plastics, which have satisfactory properties and are produced at a lower cost. They are also used as building materials and house hold commodities

for their good balance of mechanical strength. Hence, due to the increasing demands of our life style, the steadily increasing demand of plastics and plastic products leads to the rapidly growing plastics industries everywhere in the world.

A lot of efforts have been focused on the synthesis of nonlinear optical (NLO) materials in the last twenty years, because of their large application in the field of electro-optic devices such as optical information processing, telecommunication and data storage, etc. [8]. Among various polymers, polyimide (PI) is considered as the most effective polymeric material as the alignment film in LCDs because of its high thermal stability, high transition temperature (T_g), and also high orientation stability [9-11]. Polyimides are derived from both aliphatic or aromatic dianhydride and diamines, or their derivatives, and consists of heterocyclic imide in the repeat unit, which is shown in figure1.7. Some common dianhydride and common diamine are shown in figure1.8 and 1.9, respectively. The presence of $n-\pi$ conjugation between non-pair electron of nitrogen atom and π electrons of the carbonyl group makes them resistant to chemical agents and moisture.

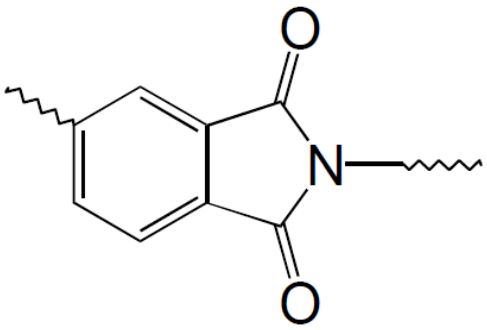

Fig.1.7 Imide linkage

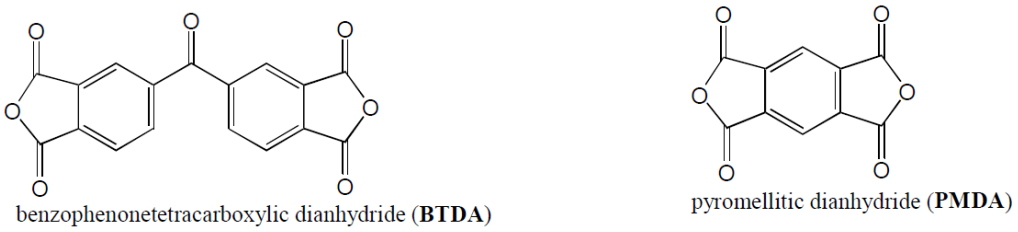

Fig. 1.8 Common dianhydride

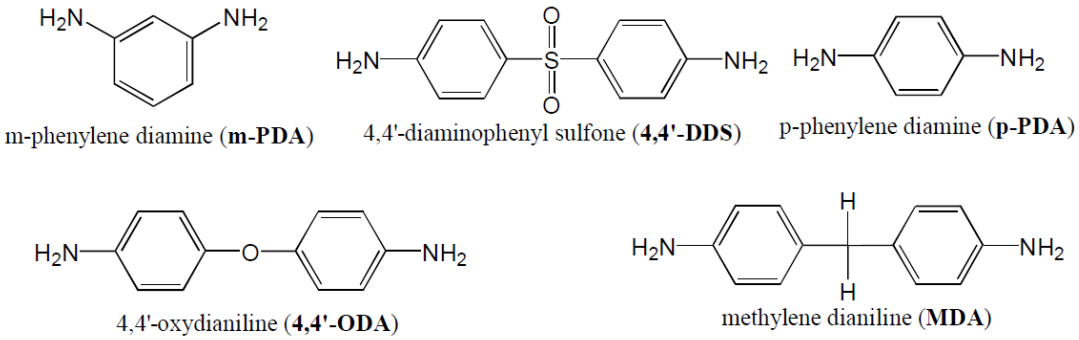

Fig.1.9 Common diamines

The basic reaction scheme of the polyimide is shown in figure 1.10, which was done in 1950's. The process produced the Kapton polyimide, and utilizes the monomer pyromellitic dianhydride (PMDA) and 4,4'-oxydianiline (ODA). Polyimides are classified according to their polymer chain, hydrocarbon residues and functional group as shown in figure 1.11. The chemical structure of the polyimides is composed of two parts: long chain polymer playing a major role for aligning LC molecules due to the rubbing effect, and chemically attached hydrocarbon branches producing a pretilt angle [12-13].

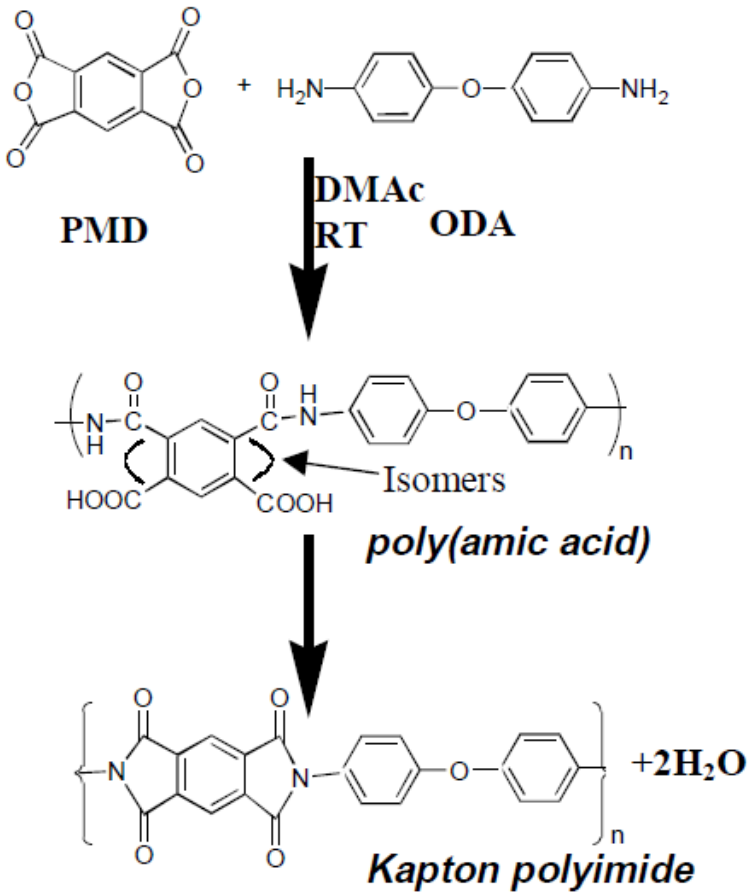

Fig.1.10 Basic reaction scheme of Kapton polyimide,

The most important characteristics of the polyimide material is their high temperature stability of the polymer. This is large advantages for the LC alignment technology. Lee *et al* reported [8] that a novel Y-type polyimide enhanced the thermal stability, which was clarified by optical second harmonic generation (SHG). In that study, they synthesized a novel Y-type polyimide (shown in figure 1.12) and observed the temporal stability of the SHG signal, and their result is shown in figure 1.13. The high thermal stability of SHG signal of polymer was due to the stability of dipole alignment of NLO chromophore.

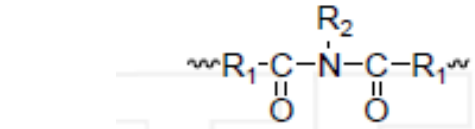

(a)

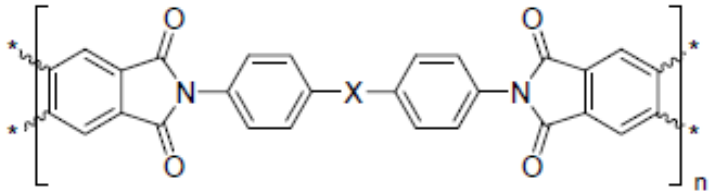

X = -O-, >C=O, >CH_2 -N=N-, -SO_2- и др.

(b)

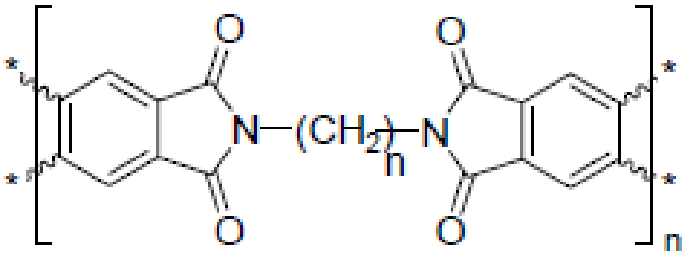

(c)

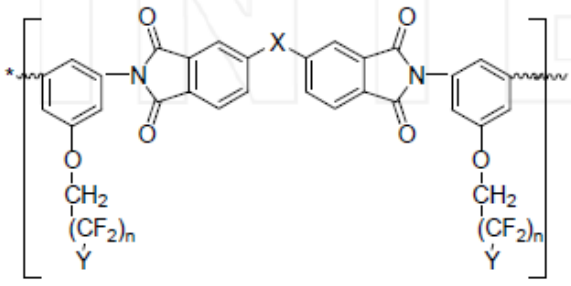

n = 1,2,3,4,5; Y= F, H

(d)

Fig.1.11 (a) linear (b) cyclic: aromatic (main-chain) (c) cyclic: aliphatic-aromatic (main-chain) and (d) Side chain

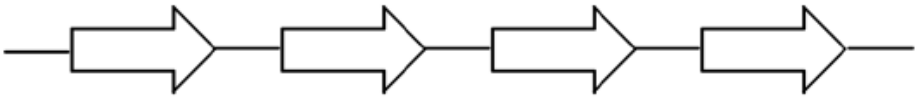

(a)

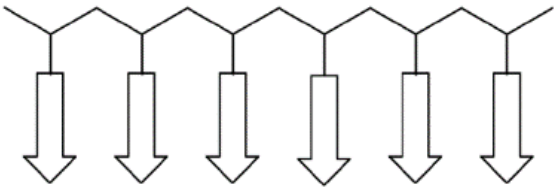

(b)

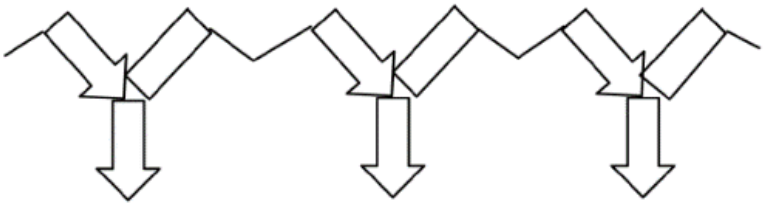

(c)

Fig. 1.12 (a) Main-chain polymers (b) side chain polymers and

(c) Y-type NLO polymers [8]

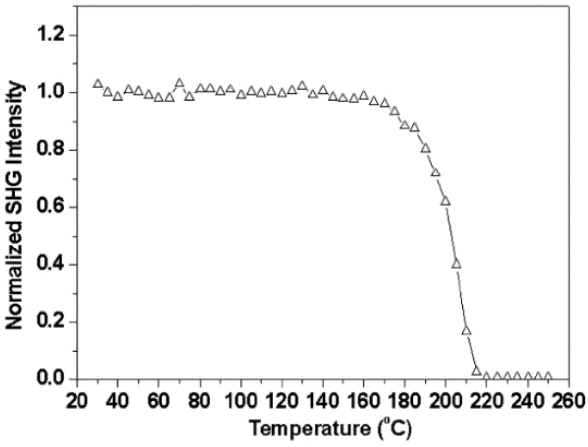

Fig. 1.13 Normalized SHG signal vs temperature at a heating rate of 10°C/min [8]

1.4 Research Motivation

The generation of the pretilt angles at the interface between alignment film and LC molecules are very significant due to the application point of view in the LCDs devices. In order to fabricate LCDs, twisted nematic (TN) LCD mode needs the pretilt angle 3 to 6^{o} [14], optically compensated bend (OCB) LCD mode needs the pretilt angle 6-10^{o} [15], and vertical alignment (VA) LCD mode requires the pretilt angle 88-90^{o} [16]. Therefore, precise control of the pretilt angle is required for the performances of LCDs.

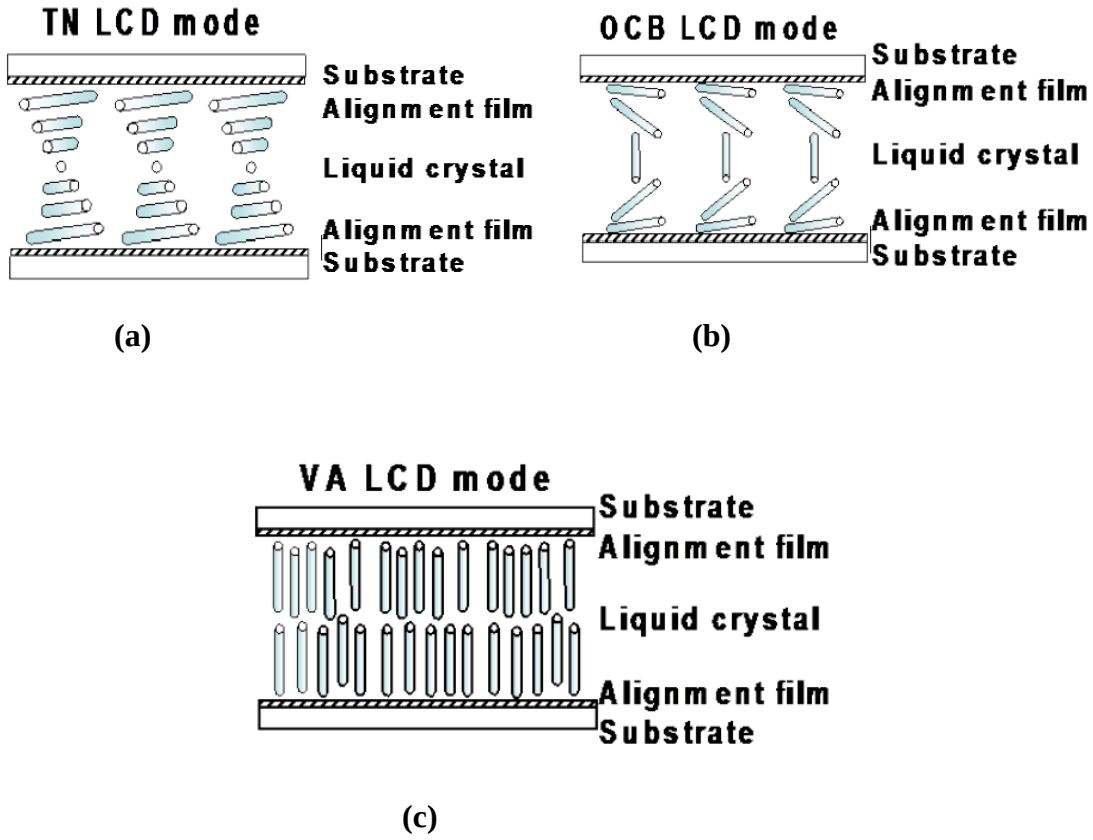

Fig. 1.14 Different LCD modes (a) Twisted nematic (TN) LCD mode (b) Optically compensated bend (OCB) LCD mode and (c) Vertical alignment (VA) LCD mode [17]

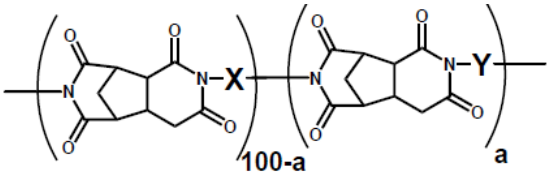

(i)

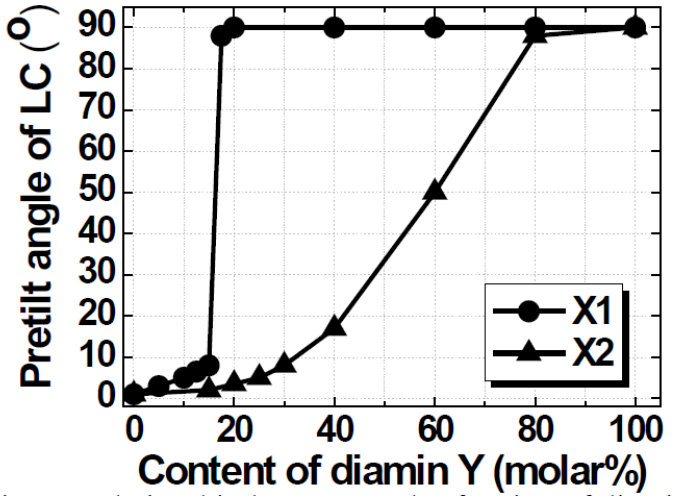

(ii)

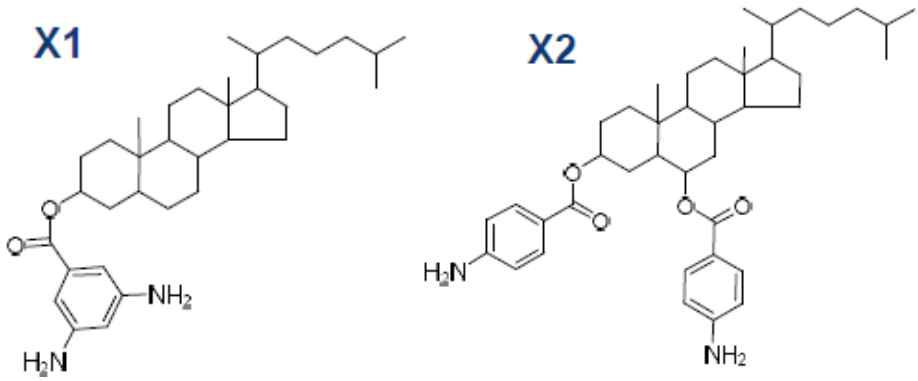

(iii)

Fig.1.15. (i) Chemical structure of PI with steroidal structure (ii) Variation of the pretilt angle with the molar fraction of diamine Y and (iii) Molecular structure of X1 and X2

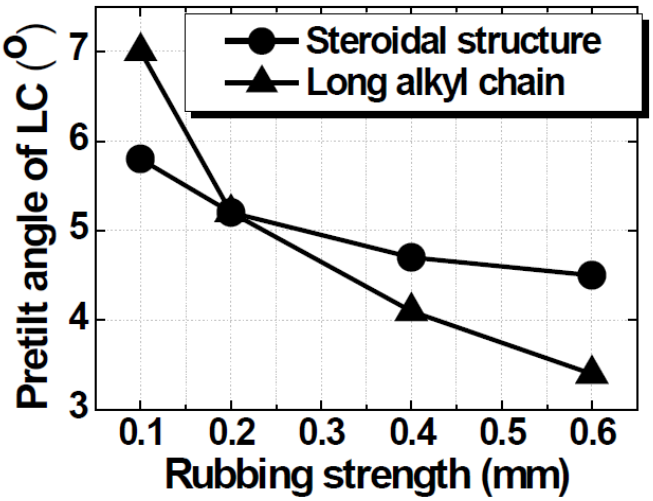

Fig. 1.16. Pretilt angle vs rubbing strength

Previously, Nishikawa [17] synthesized a novel polyimide (PI) with steroidal structure side chains having rigid chemical structure, and he used three kinds of diamine such as (a) X1: a conventional diamine with rigid structure, (b) X2: a conventional diamine with flexible structure, and (c) Y: a novel diamine with steroidal structure. The chemical structure of soluble PI with steroidal structure is shown in figure 1.15 (i). Figure 1.15 (ii) shows the variation of pretilt angle of LC with respect to the molar fraction of diamine Y, and give desired pretilt angles between 3^{o} and 90^{o}. This property is very important for different uses in LCD modes.

Figure 1.16 shows the variation of pretilt angle with respect to the rubbing strength for the PI with steroidal structure side chain and the PI with long alkyl side chain. The developed films show more stable pretilt angle (shown in figure 1.16) and higher voltage holding ratio (shown in figure 1.17) compared to a simple long alkyl chain structure. By the advantages of stability of pretilt angle and higher voltage holding ratio of this PI with steroidal structure, it is very much necessary to know the molecular orientation for the further development in LCDs device in large scale.

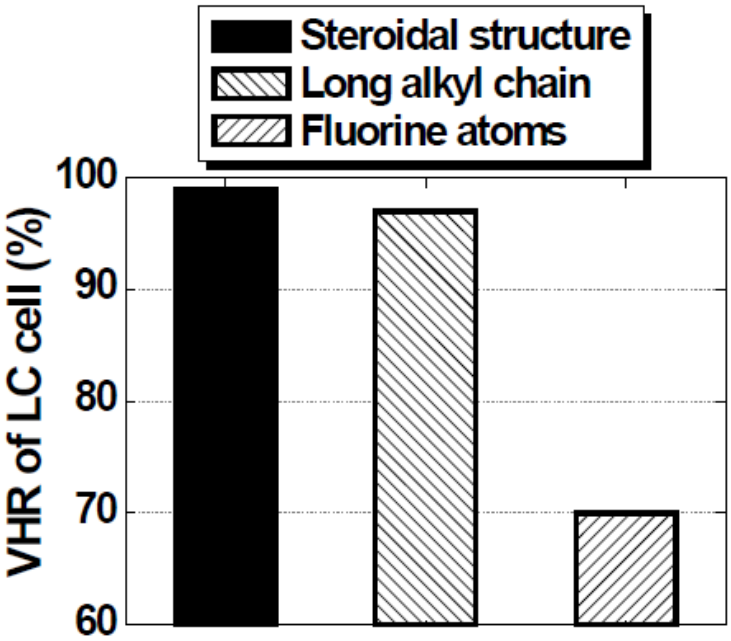

Fig. 1.17. Voltage holding ratio of LC cell for different PI

The mechanical rubbing treatment of polyimide layer, as the second important issue, using a rotating a roller which is covered by cloth with short fibers, also plays an important role for controlling the unidirectional alignment of LC molecules in the display performance of LCD panels [18-20]. The terms, l (the contact length of the rubbing roller and the substrate) are associated with stage force, roller down force and friction force. I would like to mention that there are two important mechanism occurs in the rubbing process: (i) microscopic grooves are generated in the polyimide layer during the elastic energy by the deformation of the polymer films and (ii) electrical charges produced when rubbing stress (rubbing pressure) is applied, which is the piezoelectric effect. This effect is formed the static electric field between the polymer film and roller. However, the detail of mechanism has not yet been known. There are

two important points due to the rubbing effect on the surface, such as a) periodic microgrooves, which may force the LC molecules towards the rubbing direction at the alignment surface layer, and b) van der Waals interaction, which may play a predominant role in aligning LC molecules at the interface between LCs and oriented polymer. From that point of view, it is highly important to know the orientational distribution of rubbing induced novel PI alignment layer surface with the steroidal structures. On the other hand, IR (Infrared) absorption spectrum measurement evaluates the bulk of alignment PI material, it has lack of information about surface sensitivity of the material. Previously, X-ray near edge absorption fine structure (NEXAFS), atomic force microscopy (AFM), dynamic viscoelastic measurement, and UV absorption were carried out to distinguish the rubbing effect of such long chain structures, but were not completely successful.

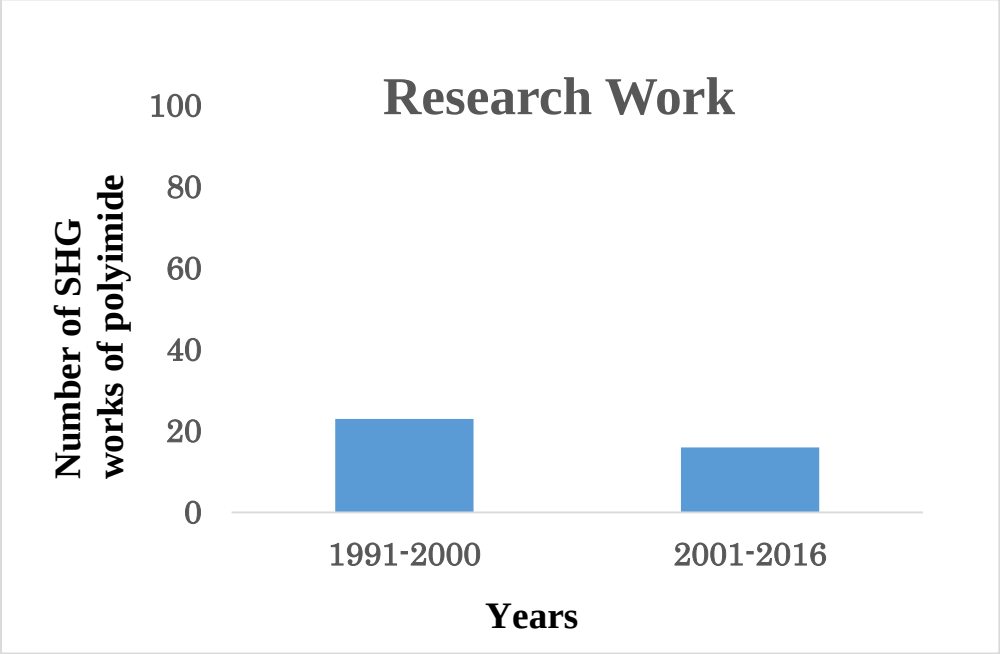

Fig. 1.18 Survey of research study of polyimide by SHG

Recently, a nonlinear optical method, in particular, second harmonic generation (SHG) is becoming a powerful technique and is largely used for studying in the field of surface and interfaces science [21-22]. In this study, in order to understand the mechanism of the rubbing effect on the surface polymer side chain, novel polyimide polymer films having steroidal structures were fabricated, and were rubbed. On the other hand, there are limited research works done on polyimide by using SHG method. I surveyed the number of research study on polyimide by SHG as shown in figure 1.18. The number of SHG works of polyimide is not big enough. In this regard, it needs a development for doing research work on polyimide alignment thin film by optical SHG for improving the performances of LCDs device. Seeing the chemical structure in figure 1.19, the part surrounded by dashed curve is the steroidal structure and is a unique component in my polyimide film. The strongest response of SHG should come from the aromatic rings in the chains. The aromatic ring of the side chain is also close and connected to the main chain of the polyimide backbone as shown in figure 1.20. Therefore, the SHG response in my experiment should also reflect the orientation of the main chain of the polymers. So far as I know, there has been no SHG measurement of polyimide polymers with steroidal structures. In addition, there is also no study about the surface orientation of the rubbed polyimide polymers with steroidal structures. Thus, my research motivation is not only analysis of the surface orientation of the rubbed novel PI with steroidal structure side chain by observing SHG response but also contribution of the SHG work of such type polyimide for the development of the research study on LCDs substrate panel.

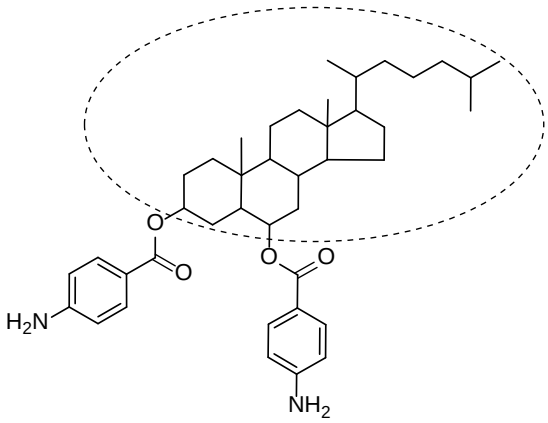

Fig. 1.19 Steroidal structure side chain (the part surrounded by dashed curve is the steroidal structure and is a unique component in our polyimide film)

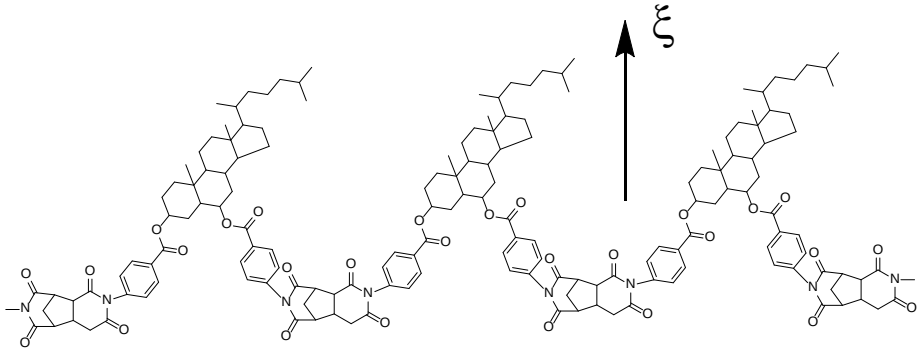

Fig.1.20 Structure of polyimide with steroid side chain

1.5 Objective of the research work

In order to understand the molecular orientation of the rubbed novel polyimide (PI) with steroidal structure side chain of diamines, an attempt has been taken to determine the nonlinear susceptibility components of rubbed PI long chains with steroidal structures and evaluate the polar (tilt) angle of the polymer chain orientation from the rotational dependence of the SHG signal. The rubbing treatment on the PI film was done by a rubbing machine and SHG response of the film was measured. Before the rubbing treatment, side chains were distributed randomly with respect to

the surface normal direction. After rubbing treatment, the side chains of polymers tend to align toward the rubbing direction with an angle from the surface normal. This is called as the tilt angle of the polymer side chain. The susceptibility elements were calculated from SHG intensity patterns. From the obtained second order nonlinear susceptibility elements, I determined the average tilt angle of the rubbed polymer with steroidal structure side chains. This is the main contribution of my thesis study. This result can be applied to develop a useful method for evaluating the liquid crystal substrate. Previously, in most reports, the amplitude of second order nonlinear susceptibility components, $|\chi_{ijk}^{(2)}|$ were considered as real values for the determination of the molecular orientation of rubbed polyimide [23-25]. However, $\chi_{ijk}^{(2)}$ has not only a real part but also imaginary part ($\mathrm{Im}\chi_{\mathrm{ijk}}^{(2)}$) because χ_{ijk} is a complex number,$\chi_{\mathrm{ijk}} = |\chi_{ijk}|\exp(ik_{ijk})$, where k_{ijk} is the phase of the χ component, which appears as a phase shift between SHG field and fundamental field. The imaginary terms,($\mathrm{Im}\chi_{\mathrm{ijk}}^{(2)}$) associated with the fluctuation of dielectric property of material. This fluctuation field will create inhomogeneous molecular orientation in the surface. Therefore, in reality, it is necessary to consider the $\chi^{(2)}$ component in the complex plane. In this regard, I analyzed the SHG patterns with the nonlinear susceptibility components in complex plane, which is a unique point in my thesis. This is also the first report in my thesis. The objectives are given as follows

a) To observe the rotation and polarization dependence of SHG signal of a novel rubbed PI with side chain diamine A (PAA-1),
b) To observe the rotation and polarization dependence of SHG signal of a novel unrubbed PI with side chain diamine A (PAA-1), and
c) To evaluate the molecular orientation of the rubbed PI with side chain diamine.

1.6 Outline of this dissertation

In chapter 1, I briefly introduced the liquid crystal, liquid crystal displays (LCDs), polyimide (PI) and the role of PI films in the alignment technology, motivation of research, and also the outline of the research.

In chapter 2, I discussed the wave equation for nonlinear source, nonlinear susceptibility, nonlinear optics, second harmonic generation, and intensity expression from of the wave equation for nonlinear source.

In chapter 3, I briefly surveyed the previous works in literature review. These are very significant review such that I can progress properly in my research work.

In chapter 4, I presented the materials synthesis process and nonlinear optical experiment.

In chapter 5, I presented the results with discussion from the both unrubbed and rubbed polyimide thin films. I also discussed the molecular orientation with respect to the rubbing treatment.

In chapter 6, I summarized the research.

References:

[1] P. J. Collings and M. Hird, “Introduction to Liquid Crystals Chemistry and Physics”, Taylor & Francis, London, (1997)

[2] S. M. Kelly, “Flat Panel Display” The Royal Society of Chemistry, Cambridge, (2000)

[3] N. Koide, The Liquid Crystal Display Story, 50 Years of Liquid Crystal R&D that lead The Way to the Future, Springer, Tokyo, (2014)

[4] J. St*ö*hr and M. G. Samant, J. Elec. Spect. Reltd. Phenm. 98-99, 189 (1999)

[5] W. F. Billmeyer, “Textbook of Polymer Science”, John Wiley and Sons, (1984)

[6] I. A. Cambel, “Introduction to synthetic polymers”, Oxford University Press, second edition, USA, (2000)

[7] Y. Lin, W. Du, D. Tu, W. Zhong, Q. Du, Polym Int. 54, 465, (2005)

[8] S. Y. Lee, S.Y. Park, H.K. Song, Polymer 47, 3540, (2006)

[9] W. T. Jung, J. Y. Lee, D. S. Won and B. K. Rhee, Polym. Int. 57, 700, (2008)

[10] K. Van den Broeck, T. Verbiest, J. Degryse, M. Van Beylan, A. Persoons, C. Samyn, Polymer 42, 3315, (2001)

[11] M.S. Kim, M.Y. Song, B. Jeon and J. Y. Lee, Mol. Cryst. Liq. Cryst. 568, 521, (2012)

[12] K. Takatoh, M. Hasegawa, M. Koden, N. Itoh, R. Hasegawa and M. Sakamoto, Taylor & Francis, New York, USA (2005)

[13] J. Y. Huang, J. S. Li, Y. S. Juang and S. H. Chen, Jpn. J. Appl. Phys. 34, 3163 (1995)

[14] M. Schadt and W. Helfrich, Appl. Phys. Lett.,18, 127, (1971)

[15] Y. Yamaguchi, T. Miyashita and T. Uchida, Tech. Dig. SID Symp. Digest 277

(1993)

[16] K. Ohmuro, S. Kataoka, T. Sasaki and Y. Koike, Tech. Dig. SID Symp. Digest 845, (1997)

[17] M. Nishikawa, T. Miyamoto, S. Kawamura, Y. Tsuda, N. Bessho, D.-S. Seo, Y. Iimura, and S. Kobayashi, Mol. Cryst. Liq. Cryst. 258, 285, (1995)

[18] T. Sakai, K. Ishikawa and H. Takezoe, Liquid Crystal 29(1), 47, (2002)

[19] T. Sakai, J. G. Yoo, Y. Kinoshita, K. Ishikawa, H. Takezoe, A. Fukuda, T. Nihira and H. Endo, Appl. Phys. Lett. 71(16), 2274, (1997).

[20] S.C. Hong, M. Oh-e, X. Zhuang and Y. R. Shen, Phys. Rev. E 63, 051706, (2001).

[21] H. Sano, J. Saito, J. Ikeda and G. Mizutani, J. Appl. Phys. 100, 043710, (2006).

[22] A. B. El Basaty, Y. Miyauchi, G. Mizutani, T. Matsushima and H. Murata, Appl. Phys. Lett. 97, 193302, (2010)

[23] Jason et al, J. Am. Chem. Soc. 123, 5768, (2001)

[24] S.C. Hong, M. Oh-e, X. Zhuang ,Y. R. Shen, J. J. Ge, F. W. Harris and S. Z. D. Cheng, Phys. Rev. E 63**,** 051706 (2001)

[25] K. Shirota, K. Ishikawa, H. Takezoe, A. Fukuda and T. Shibashi, Jpn. J. Appl. Phys. 34, Pt. 2, No. 3A, L316 (1995)

Chapter 2

GENERAL THEORY

2.1 The wave equation for nonlinear source

The wave equation can be obtained for the propagation of light through a nonlinear optical medium by using Maxwell's equation [1].

$$\vec{\nabla} \times \vec{\mathrm{E}} = -\frac{\partial \vec{\mathrm{B}}}{\partial \mathrm{t}} \tag{2.1}$$

$$\vec{\nabla} \times \vec{\mathrm{H}} = \frac{\partial \vec{\mathrm{D}}}{\partial \mathrm{t}} + \vec{\mathrm{J}} \tag{2.2}$$

where $\vec{\mathrm{E}}$ and $\vec{\mathrm{B}}$ are the electric field and magnetic induction, respectively. $\vec{\mathrm{D}}$, $\vec{\mathrm{H}}$ and $\vec{\mathrm{J}}$ are the electric displacement, magnetic field strength and current density, respectively. $\vec{D}$ and $\vec{E}$ are also related by

$$\vec{\mathrm{D}} = \varepsilon_o \vec{\mathrm{E}} + \vec{\mathrm{P}} \tag{2.3}$$

where $\vec{\mathrm{P}}$ is the induced polarization and assume that , $\vec{\mathrm{J}}$ =0 for charge free space. Taking the curl into the both-side of equation (2.1), and using equation (2.2) with $\vec{B} = \vec{\mathrm{H}}$

$$\vec{\nabla} \times \vec{\nabla} \times \vec{\mathrm{E}} + \frac{\partial^2}{\partial \mathrm{t}^2} \vec{\mathrm{D}} = 0 \tag{2.4}$$

Now using the equation (2.3) and obtain the desire equation,

$$\vec{\nabla} \times \vec{\nabla} \times \vec{\mathrm{E}} + \varepsilon \frac{\partial^2}{\partial \mathrm{t}^2} \vec{\mathrm{E}} = - \frac{\partial^2}{\partial \mathrm{t}^2} \vec{P}^{NL} \tag{2.5}$$

This is called the general form of the wave equation in nonlinear optics.

It is convenient to split $\vec{P}$ into its linear and nonlinear parts as

$$\vec{P} = \vec{P}^{(1)} + \vec{P}^{NL} \tag{2.6}$$

where $\vec{P}^{(1)}=\varepsilon_0\chi\vec{E}$, it belongs to linear relationship between $\vec{P}^{(1)}$ and $\vec{E}$. When the electric field strength is strong enough, the linear relationship is no longer hold, the induced nonlinear polarization becomes [2]

$$\vec{P} = \varepsilon_0\chi\vec{E} + \varepsilon_0\chi^{(2)}:\vec{E}.\vec{E} + \varepsilon_0\chi^{(3)} \vdots \vec{E}.\vec{E}.\vec{E} + \ldots\ldots .. \tag{2.7}$$

where $\chi^{(2)}$ and $\chi^{(3)}$ are the second and third order nonlinear optical susceptibilities, respectively.

2.2 Nonlinear susceptibility: Classical anharmonic oscillator model

Let assume that the medium is noncentrosymmetric, which gives rise to a second order nonlinear optical susceptibility. The equation of motion of the electron coordinate x can write in the following form:

$$m\frac{d^2x}{dt^2} + 2m\gamma\frac{dx}{dt} + m\omega_o^2x + ax^2 + bx^3 + \cdots = -\lambda e\vec{E}(t) \tag{2.8}$$

where ω_o is the oscillation frequency of the electron, m= the mass of electron, γ=the damping factor, and ax^2 and bx^3 are denote the nonlinear terms. λ is the expansion parameter, which characterizes the strength of the perturbation..

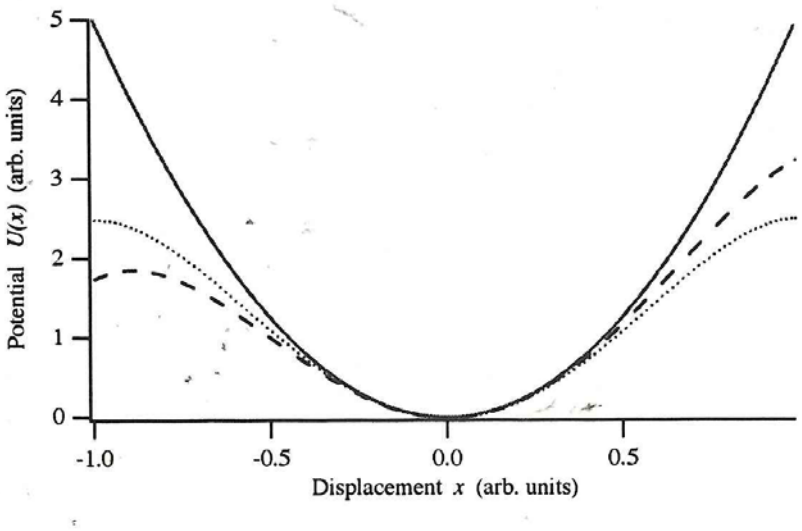

Fig.2.1 Potential Curves for different form of restoring force [3]

Then the equation (2.8) can also be written as

$$\frac{d^2x}{dt^2} + 2\gamma\frac{dx}{dt} + \omega_o^2 x + (a/m)x^2 + (b/m)x^3 + \cdots = -\lambda e\vec{E}(t)/m \qquad (2.9)$$

Let the applied field $E(t) = E^{(1)} = E^{\omega}\exp(-i\omega t)$ (2.10)

and consider that $x = x^{(1)} = x^{\omega}\exp(-i\omega t)$ (2.11)

The equation (2.9) is written in the form of a power series expansion of λ as followings

$$\lambda\ddot{x}^{(1)} + \lambda^2\ddot{x}^{(2)} + 2\gamma(\lambda\dot{x}^{(1)} + \lambda^2\dot{x}^{(2)}) + \omega_o^2(\lambda x^{(1)} + \lambda^2 x^{(2)}) + a/m(\lambda x^{(1)} +$$

$$\lambda^2 x^{(2)})^2 + b/m(\lambda x^{(1)} + \lambda^2 x^{(2)})^3 + \cdots = -\lambda e\vec{E}(t)/m \qquad (2.12)$$

Comparing the coefficient of λ in (2.12)

$$\ddot{x}^{(1)} + 2\gamma\dot{x}^{(1)} + \omega_o^2 x^{(1)} = -e\vec{E}(t)/m \qquad (2.13)$$

Putting the equations (2.10) and (2.11) into (2.13) for the first order of λ, and solving that

$$x^{(1)}= \frac{e}{m}\frac{E^{(1)}}{\omega_o^2-\omega^2-i2\gamma\omega} \tag{2.14}$$

Now comparing the coefficient of λ^2

$$\ddot{x}^{(2)} + 2\gamma\dot{x}^{(2)} + \omega_o^2 x^{(2)} + a/m(x^{(1)})^2 = 0 \tag{2.15}$$

Let $x^{(2)}=x^{2\omega}\exp(-i2\omega t)$ (2.16)

Substituting (2.15) into equation (2.14), I get,

$$x^{(2)} = -\frac{ae^2}{m^2}\ \frac{(E^{\omega})^2\exp(-i2\omega t)}{[\omega_o^2-\omega^2-i2\gamma\omega]^2}\ \frac{1}{[\omega_o^2-4\omega^2-i4\gamma\omega]} \tag{2.17}$$

The linear susceptibility is given by

$$\vec{P}^{(1)}=\varepsilon_0\chi^{(1)}\vec{E}(t) \tag{2.18}$$

Then linear polarization is

$$\vec{P}^{(1)} = -Ne x^{(1)} \tag{2.19}$$

Thus, the linear susceptibility

$$\chi^{(1)} = \frac{Ne^2}{\varepsilon_o m}\left(\frac{1}{\omega_o^2-\omega^2-i2\gamma\omega}\right) \tag{2.20}$$

The second order nonlinear polarization is

$$\vec{P}^{(2)}= \varepsilon_0\chi^{(2)}\vec{E}^2(t) \tag{2.21}$$

Similarly, the desired the second order nonlinear susceptibility is

$$\chi^{(2)} = \frac{Neae^2}{\varepsilon_o m^2} \frac{1}{[\omega_o^2 - \omega^2 - i2\gamma\omega]^2} \frac{1}{[\omega_o^2 - 4\omega^2 - i4\gamma\omega]} \quad (2.22)$$

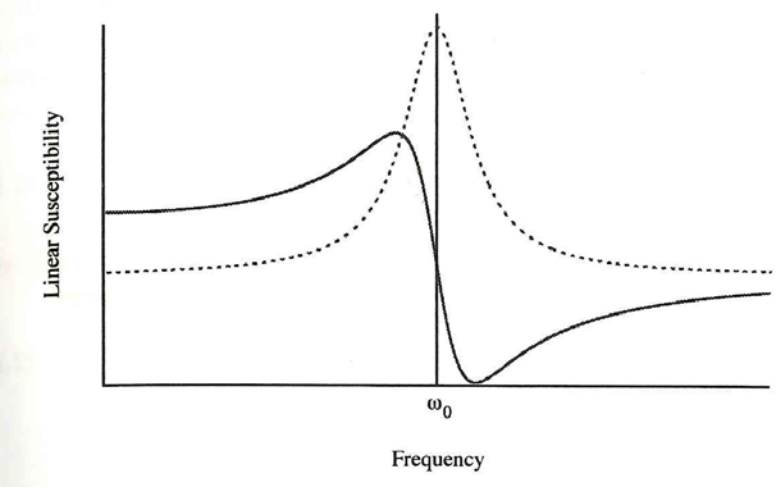

Fig.2.2 Linear dielectric constant vs frequency [3]

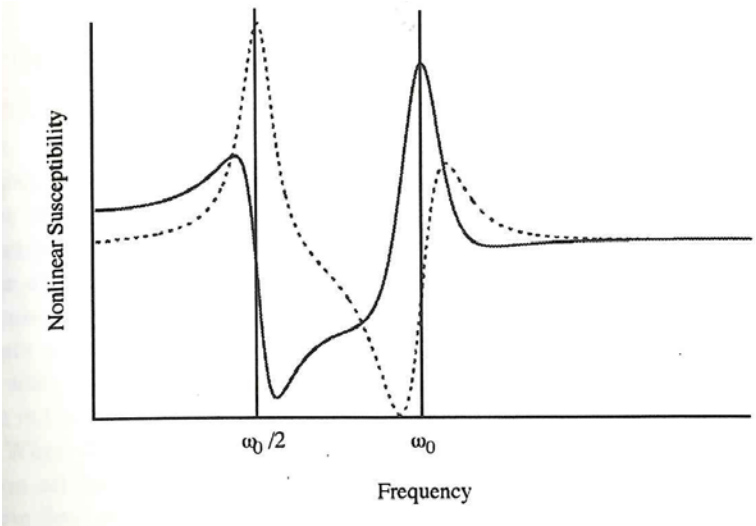

Fig.2.3 nonlinear susceptibility vs frequency [3]

2.3 Nonlinear optics: Second harmonic generation

Second harmonic generation (SHG) is the second order nonlinear optical process where two photons at the same frequency (ω) are converted into a photon at the second harmonic frequency (2ω) [2].

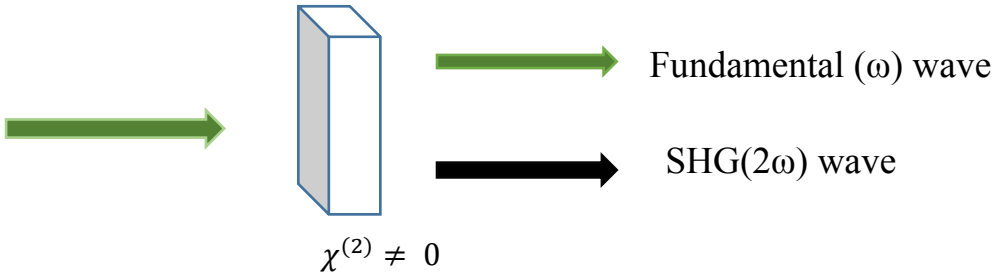

Fig.2.4. SHG wave

If we consider that the electric field is incident on the crystal for which the second order nonlinear susceptibility is non zero ($\chi^{(2)} \neq 0$).

$$\vec{E}(t) = Eexp(-i\omega t) + c.c. \tag{2.23}$$

Putting the equation (2.21) into equation (2.23), we obtain,

$$\vec{P}^{(2)}(t) = 2\chi^{(2)}EE^{*} + (\chi^{(2)}E^{2}\exp(-2i\omega t) + c.c) \tag{2.24}$$

The first term of equation (25) in right hand side denotes the optical rectification in which a static electric field is created in the nonlinear crystal. The second terms in the right hand side generate the radiation of second harmonic frequency at 2ω. In order to find the electric field expression for SHG wave, we consider that the propagation of electric fields for ω and 2ω in air along the direction of z

$$\vec{E}_{\omega}(z,t) = E_{\omega 0} \exp\left(-\frac{\kappa_{\omega}^{air}\omega z}{c}\right) \exp\{i\left(\frac{\omega n_{\omega}^{air} z}{c} - \omega t\right)\} \quad (2.25)$$

and $\vec{E}_{2\omega}(z,t) = E_{2\omega 0} \exp\left(-\frac{\kappa_{2\omega}^{air}\omega z}{c}\right) \exp\{i\left(\frac{2\omega n_{2\omega}^{air} z}{c} - 2\omega t\right)\}$ (2.26)

where the wave vector at the fundamental wave, $k_{\omega} = \frac{\omega n_{\omega}^{air}}{c}$ and the wave vector at the SHG wave, $k_{2\omega} = \frac{2\omega n_{2\omega}^{air}}{c}$, n_{ω}^{air} and $n_{2\omega}^{air}$ are the normal refractive index for ω and 2ω, respectively, in air. κ_{ω}^{air} and $\kappa_{2\omega}^{air}$ are the imaginary part of the refractive index for ω and 2ω, respectively, in air. If the medium is very weakly absorbing, then we can assume that κ is very small ($\kappa_{\omega}^{air} \approx 0$ & $\kappa_{2\omega}^{air} \approx 0$);

Therefore, the propagation of electric fields for ω and 2ω in air becomes

$$\vec{E}_{\omega}(z,t) = E_{\omega 0} \exp\{i(k_{\omega} z - \omega t)\} \quad (2.27)$$

$$\vec{E}_{2\omega}(z,t) = E_{2\omega 0} \exp\{i(k_{2\omega} z - 2\omega t)\} \quad (2.28)$$

2.4 Derivation of intensity expression from a second harmonic wave

Let us consider that the propagation of a plane wave along the direction of z with nonlinear source $\vec{P}^{NL}$,

Case-I: Fundamental wave,

$$\frac{\partial^2 \vec{E}_{\omega_1}}{\partial z^2} + k_{\omega}^2 \vec{E}_{\omega_1} = -\frac{4\pi\omega_1^2}{c^2} \vec{P}_{\omega_1}^{NL}(z) \quad (2.29)$$

Case-II: SHG wave

$$\frac{\partial^2\vec{E}_{\omega_2}}{\partial z^2} + k_{2\omega}^2\vec{E}_{\omega_2} = -\frac{4\pi\omega_2^2}{c^2}\vec{P}_{\omega_2}^{NL}(z) \quad (2.30)$$

Let the solution of the form

$$\vec{E}_{\omega_1} = \vec{A}_{\omega}(z)e^{ik_{\omega}z} \quad (2.31)$$

and $\vec{E}_{\omega_2} = \vec{A}_{2\omega}(z)e^{ik_{2\omega}z}$ (2.32)

where, $\vec{A}_{\omega}$ and $\vec{A}_{2\omega}$ are the slowly varying electric field amplitude of wave at fundamental and SHG wave , respectively. Using equation (2.32) into equation (2.30) ,

we obtain,

$$\frac{\partial^2\vec{A}_{\omega}(z)}{\partial z^2} + 2ik_{\omega}\frac{\partial\vec{A}_{\omega}(z)}{\partial z} = -\frac{4\pi\omega_1^2}{c^2}\vec{P}_{\omega_1}^{NL}(z)\, e^{-ik_{\omega}z} \quad (2.33)$$

The slowly varying amplitude approximation: $\left|\frac{\partial^2\vec{A}_{\omega}(z)}{\partial z^2}\right| \ll \left|2k\frac{\partial\vec{A}_{\omega}(z)}{\partial z}\right|$, from equation (2.33), one obtain,

$$\frac{\partial\vec{A}_{\omega}(z)}{\partial z} = \frac{2i\pi\omega_1^2}{k_{\omega}c^2}\vec{P}_{\omega_1}^{NL}(z)e^{-ik_{\omega}z} \quad (2.34)$$

Similarly, $\frac{\partial\vec{A}_{2\omega}(z)}{\partial z} = \frac{2i\pi\omega_2^2}{k_{2\omega}c^2}\vec{P}_{\omega_2}^{NL}(z)e^{-ik_{2\omega}z}$ (2.35)

The nonlinear polarization is represented as

$$\vec{P}_{\omega_1}^{NL}(z) = 4d\vec{E}_{\omega_2}\vec{E}_{\omega_1}^{*} = 4d\vec{A}_{2\omega}\vec{A}_{\omega}^{*}e^{i(k_{2\omega}-k_{\omega})z} \quad (2.36)$$

and $\vec{P}_{\omega_2}^{NL}$ (z) $= 2\mathrm{d}\vec{E}_{\omega_1}^{2} = 2d\vec{A}_{\omega}^{2}e^{2ik_{\omega}z}$ (2.37)

Using equation (2.36) and (2.37) into equation (2.34) and (2.35), respectively. Therefore, we get two coupled amplitude equations become,

$$\frac{\partial\vec{A}_{\omega}(z)}{\partial z} = \frac{8\pi i\omega_1^2 d}{k_{\omega}c^2}\vec{A}_{2\omega}\vec{A}_{\omega}^{*}e^{-i\Delta kz} \quad (2.38)$$

and $$\frac{\partial\vec{A}_{2\omega}(z)}{\partial z} = \frac{4\pi i\omega_2^2 d}{k_{2\omega}c^2}\vec{A}_{\omega}^{2}e^{i\Delta kz} \quad (2.39)$$

where, $\Delta k = 2k_{\omega}\text{-}k_{2\omega}$ (2.40)

Now, integrating the equations (2.38) and (2.40) from z = 0 to z = L, I get

$$\vec{\mathrm{A}}_{\omega} = \frac{8\pi\mathrm{i}\omega_1^2\mathrm{d}}{\mathrm{k}_{\omega}\mathrm{c}^2}\vec{\mathrm{A}}_{2\omega}\vec{\mathrm{A}}_{\omega}^{*}\int_{\mathrm{o}}^{\mathrm{L}}\mathrm{e}^{-\mathrm{i}\Delta\mathrm{kz}}\,\mathrm{dz}$$

$$= \frac{8\pi\mathrm{i}\omega_1^2\mathrm{d}}{\mathrm{k}_{\omega}\mathrm{c}^2}\vec{\mathrm{A}}_{2\omega}\vec{\mathrm{A}}_{\omega}^{*}\frac{\left(\mathrm{e}^{-\mathrm{i}\Delta\mathrm{kL}}-1\right)}{-\mathrm{i}\Delta\mathrm{k}}$$

$$= -\frac{8\pi\omega_1^2\mathrm{d}}{\mathrm{k}_{\omega}\mathrm{c}^2}\vec{\mathrm{A}}_{2\omega}\vec{\mathrm{A}}_{\omega}^{*}\frac{\left(\mathrm{e}^{-\mathrm{i}\Delta\mathrm{kL}}-1\right)}{\Delta\mathrm{k}} \quad (2.41)$$

and

$$\vec{\mathrm{A}}_{2\omega} = \frac{4\pi\mathrm{i}\omega_2^2\mathrm{d}}{\mathrm{k}_{2\omega}\mathrm{c}^2}\vec{\mathrm{A}}_{\omega}^{2}\int_{\mathrm{o}}^{\mathrm{L}}\mathrm{e}^{\mathrm{i}\Delta\mathrm{kz}}\,\mathrm{dz}$$

$$= \frac{4\pi\mathrm{i}\omega_2^2\mathrm{d}}{\mathrm{k}_{2\omega}\mathrm{c}^2}\vec{\mathrm{A}}_{\omega}^{2}\frac{\left(\mathrm{e}^{\mathrm{i}\Delta\mathrm{kL}}-1\right)}{\mathrm{i}\Delta\mathrm{k}}$$

$$= \frac{4\pi\omega_2^2 d}{k_{2\omega}c^2}\vec{A}_\omega^2 \frac{(e^{i\Delta kL}-1)}{\Delta k} \quad (2.42)$$

Therefore, the electric fields are given by

$$\vec{E}_{\omega_1} = -\frac{8\pi\omega_1^2 d}{k_\omega c^2}\vec{A}_{2\omega}\vec{A}_\omega^* \frac{(e^{-i\Delta kL}-1)}{\Delta k} e^{ik_\omega z} \quad (2.43)$$

$$\vec{E}_{\omega_2} = \frac{4\pi\omega_2^2 d}{k_{2\omega}c^2}\vec{A}_\omega^2 \frac{(e^{i\Delta kL}-1)}{\Delta k} e^{ik_{2\omega} z} \quad (2.44)$$

Therefore, the intensity of the SHG wave is given by

$$I_{SHG} = \frac{n_{2\omega}c}{2\pi}\left|\vec{A}_{2\omega}\right|^2 = \frac{8\pi n_{2\omega}\omega_2^4 d^2}{k_{2\omega}^2 c^3}|\vec{A}_\omega^2|^2 \left|\frac{(e^{i\Delta kL}-1)}{\Delta k}\right|^2 \quad (2.45)$$

or $$I_{SHG} = \frac{4\pi\omega_2^2}{n_{2\omega}c}|\chi^{(2)}|^2 I_\omega^2 \left|\frac{(e^{i\Delta kL}-1)}{\Delta k}\right|^2$$

or $$I_{SHG} = \frac{16\pi\omega^2}{n_{2\omega}c}|\chi^{(2)}|^2 I_\omega^2 \left|\frac{(e^{i\Delta kL}-1)}{\Delta k}\right|^2 \quad (2.46)$$

where , $I_\omega = \vec{A}_\omega^2$ and $d^2 = \frac{1}{2}|\chi^{(2)}|^2$

But, $\left|\frac{(e^{i\Delta kL}-1)}{\Delta k}\right|^2 = L^2 \frac{\sin^2(\Delta kL/2)}{(\Delta kL/2)^2}$

Therefore the SHG intensity is given by the following relation:

$$I_{SHG} = \frac{16\pi\omega^2}{n_{2\omega}c}|\chi^{(2)}|^2 I_\omega^2 \; L^2 \frac{\sin^2(\Delta kL/2)}{(\Delta kL/2)^2} \quad (2.47)$$

or $$I_{SHG} \propto |\chi^{(2)}|^2 I_\omega^2 \quad (2.48)$$

2.5 Theory of molecular orientation distribution

Consider that N_s is a number of molecules per unit surface with molecular hyper-polarizability, $\overleftrightarrow{\beta}$, and the following relation is given by [3]

$$\overleftrightarrow{\chi}_s^{(2)} = \frac{1}{\varepsilon_o}\sum_i N_s \langle \overleftrightarrow{T}_i \rangle \ \overleftrightarrow{\beta}_i \tag{2.49.a}$$

$\overleftrightarrow{\chi}_s^{(2)}$ is the macroscopic susceptibility tensor of the surface, $\overleftrightarrow{T}_i$ is the transformation tensor of molecular type i. I used an ensemble average because a large number of molecules of type i to participate in this process. I can use the angle distribution function as follows.

$$< T > = \int f\,(\phi, \theta, \psi)\, T(\phi, \theta, \psi) d\Omega \tag{2.49.b}$$

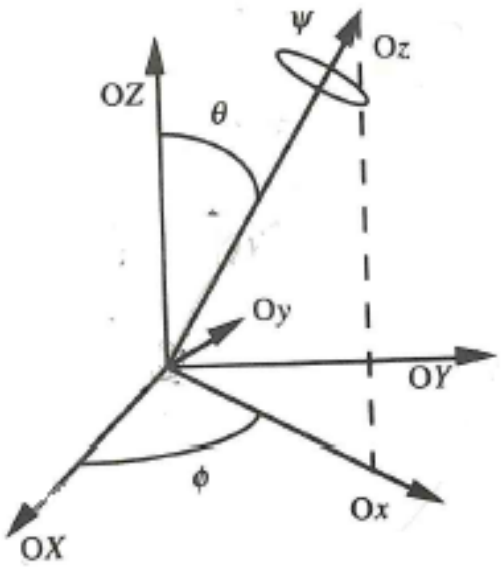

Fig. 2.5 Reference frames: laboratory coordinate and molecular coordinate [3]

where the subscript is omitted for simplicity, $f(\phi,\theta,\psi)$ is the probability of finding a molecule with a value between ϕ and $\phi + d\phi$, θ and $\theta + d\theta$ and ψ and $\psi + d\psi$. For any adsorbed molecule, the transformation law is applicable, which as shown in equation (2.49). The macroscopic nonlinear tensor has a few nonzero independent elements, such as $\chi^{(2)}_{s,XZX}$, $\chi^{(2)}_{s,ZXX}$, $\chi^{(2)}_{s,ZZZ}$ and $\chi^{(2)}_{s,XXZ}$.

The molecular frame is related with the laboratory frame through the three Euler angles ϕ, θ and ψ, where ϕ is the angle of rotation around the surface normal , θ is the angle between the surface normal and the molecular axis, and ψ is the angle of rotation around the molecular axis. I define these three rotations as follows

$$A_\phi = \begin{bmatrix} cos\phi & -sin\phi & 0 \\ sin\phi & cos\phi & 0 \\ 0 & 0 & 1 \end{bmatrix} \tag{2.50}$$

$$A_\theta = \begin{bmatrix} 1 & 0 & 0 \\ 0 & cos\theta & -sin\theta \\ 0 & sin\theta & cos\theta \end{bmatrix} \tag{2.51}$$

and

$$A_\psi = \begin{bmatrix} cos\psi & -sin\psi & 0 \\ sin\psi & cos\psi & 0 \\ 0 & 0 & 1 \end{bmatrix} \tag{2.52}$$

The transformation from the laboratory frame to the molecular frame is given by

$$T = (A_\psi A_\theta A_\phi)^{-1} \tag{2.53}$$

Therefore, the reverse transformation, which is interested, and is given by

$$T = (A_\psi A_\theta A_\phi) \tag{2.54}$$

$$= \begin{bmatrix} cos\psi & -sin\psi & 0 \\ sin\psi & cos\psi & 0 \\ 0 & 0 & 1 \end{bmatrix} \begin{bmatrix} 1 & 0 & 0 \\ 0 & cos\theta & -sin\theta \\ 0 & sin\theta & cos\theta \end{bmatrix} \begin{bmatrix} cos\phi & -sin\phi & 0 \\ sin\phi & cos\phi & 0 \\ 0 & 0 & 1 \end{bmatrix}$$

$$= \begin{bmatrix} cos\psi & -sin\psi cos\theta & sin\psi sin\theta \\ sin\psi & cos\psi cos\theta & -cos\psi sin\theta \\ 0 & sin\theta & cos\theta \end{bmatrix} \begin{bmatrix} cos\phi & -sin\phi & 0 \\ sin\phi & cos\phi & 0 \\ 0 & 0 & 1 \end{bmatrix}$$

Thus,

$$\mathrm{T} = \begin{bmatrix} cos\psi cos\phi - sin\psi cos\theta sin\phi & -cos\psi sin\phi - sin\psi cos\theta cos\phi & sin\psi sin\theta \\ sin\psi cos\phi + cos\psi cos\theta sin\phi & -sin\psi sin\phi + cos\psi cos\theta cos\phi & -cos\psi sin\theta \\ sin\theta sin\phi & sin\theta cos\phi & cos\theta \end{bmatrix} \tag{2.55}$$

If I assume that molecules have one dominant molecular susceptibility component along the long molecular axis z, i.e. β_{zzz}. The macroscopic elements are as follows along the molecular axis z,

$$\chi^{(2)}_{s,ZZZ} = \frac{N_s}{\varepsilon_o} < T^{zzz}_{ZZZ} > \beta_{zzz} = \frac{N_s}{\varepsilon_o} < cos^3\theta > \beta_{zzz} \tag{2.56}$$

$$\chi^{(2)}_{s,XZX} = \frac{N_s}{\varepsilon_o} < T^{zzz}_{XZX} > \beta_{zzz} = \frac{N_s}{\varepsilon_o} < sin^2\psi sin^2\theta cos\theta > \beta_{zzz} \tag{2.57}$$

$$\chi^{(2)}_{s,XXX} = \frac{N_s}{\varepsilon_o} < T^{zzz}_{XXX} > \beta_{zzz} = \frac{N_s}{\varepsilon_o} < sin^3\psi sin^3\theta > \beta_{zzz} \tag{2.58}$$

$$\chi^{(2)}_{s,ZXX} = \frac{N_s}{\varepsilon_o} < T^{zzz}_{ZXX} > \beta_{zzz} = \frac{N_s}{\varepsilon_o} < sin^2\psi sin^2\theta cos\theta > \beta_{zzz} \tag{2.59}$$

$$\chi^{(2)}_{s,ZXZ} = \frac{N_s}{\varepsilon_o} < T^{zzz}_{ZXZ} > \beta_{zzz} = \frac{N_s}{\varepsilon_o} < sin\psi cos^2\theta sin\theta > \beta_{zzz} \tag{2.60}$$

$$\chi^{(2)}_{s,ZYY} = \frac{N_s}{\varepsilon_o} < T^{zzz}_{ZYY} > \beta_{zzz} = \frac{N_s}{\varepsilon_o} < cos\theta cos^2\psi sin^2\theta > \beta_{zzz} \quad (2.61)$$

$$\chi^{(2)}_{s,XYY} = \frac{N_s}{\varepsilon_o} < T^{zzz}_{XYY} > \beta_{zzz} = \frac{N_s}{\varepsilon_o} < sin\psi cos^2\psi sin^3\theta > \beta_{zzz} \quad (2.62)$$

These equation are employed to analyze the molecular orientation. In the case of Dirac delta distribution function, which is centered on ψ = 0º or ψ = 90º. On the other hand, the angle, θ becomes important parameter, because it receive a more detail information in the molecular orientation. It gives the angle between the molecular axis and surface or interface normal. Therefore the equations 2.56 to 2.62 in terms of θ are as follow.

$$\chi^{(2)}_{s,ZZZ} = \frac{N_s}{\varepsilon_o} < cos^3\theta > \beta_{zzz} \quad (2.63)$$

$$\chi^{(2)}_{s,XZX} = \frac{N_s}{\varepsilon_o} < sin^2\theta cos\theta > \beta_{zzz} \quad (2.64)$$

$$\chi^{(2)}_{s,XXX} = \frac{N_s}{\varepsilon_o} < sin^3\theta > \beta_{zzz} \quad (2.65)$$

$$\chi^{(2)}_{s,ZXX} = \frac{N_s}{\varepsilon_o} < sin^2\theta cos\theta > \beta_{zzz} \quad (2.66)$$

$$\chi^{(2)}_{s,ZXZ} = \frac{N_s}{\varepsilon_o} < cos^2\theta sin\theta > \beta_{zzz} \quad (2.67)$$

$$\chi^{(2)}_{s,ZYY} = \frac{N_s}{\varepsilon_o} < cos\theta sin^2\theta > \beta_{zzz} \quad (2.68)$$

$$\chi^{(2)}_{s,XYY} = \frac{N_s}{\varepsilon_o} < sin^3\theta > \beta_{zzz} \quad (2.69)$$

From (2.63) and (2.65) , I can write

$$tan^3\theta = \chi^{(2)}_{s,XXX} \Big/ \chi^{(2)}_{s,ZZZ} \tag{2.70}$$

From (2.65) and (2.67), I can write,

$$tan^2\theta = \chi^{(2)}_{s,XXX} \Big/ \chi^{(2)}_{s,ZXZ} \tag{2.71}$$

From (2.65) and (2.66), I can write,

$$tan\theta = \chi^{(2)}_{s,XXX} \Big/ \chi^{(2)}_{s,ZXX} \tag{2.72}$$

Now, I can use these equations (2.70 to 2.72), in order to get the desired tilt angle i.e. molecular orientation with knowing the $\chi^{(2)}_{s,XXX}$, $\chi^{(2)}_{s,ZZZ}$, $\chi^{(2)}_{s,ZXZ}$ and $\chi^{(2)}_{s,ZXX}$ in complex plane.

References:

[1] A. Yariv, “Quantum Electronics” 3rd edition, John Wiley & Sons, New York (1989)

[2] R. W. Boyd, “Nonlinear Optics” Academic Press, Inc., London, (1992)

[3] P. F. Brevet, Surface Second Harmonic Generation, Press polytechniques et universitaires romandes (PPUR) (1996)

Chapter 3
Literature Review

3.1 Curing temperature, imidization ratio and dichroic ratio

Curing temperature is one of the most important parameters to improve the fabrication of full colour liquid crystal displays (LCDs). Conventional polymeric polyimide (PI) material required curing temperatures above 250^{o}C , which is not suitable for the fabrication of full color LCD because the color filter containing organic pigments or dyes are not stable above 200^{o}C [1].

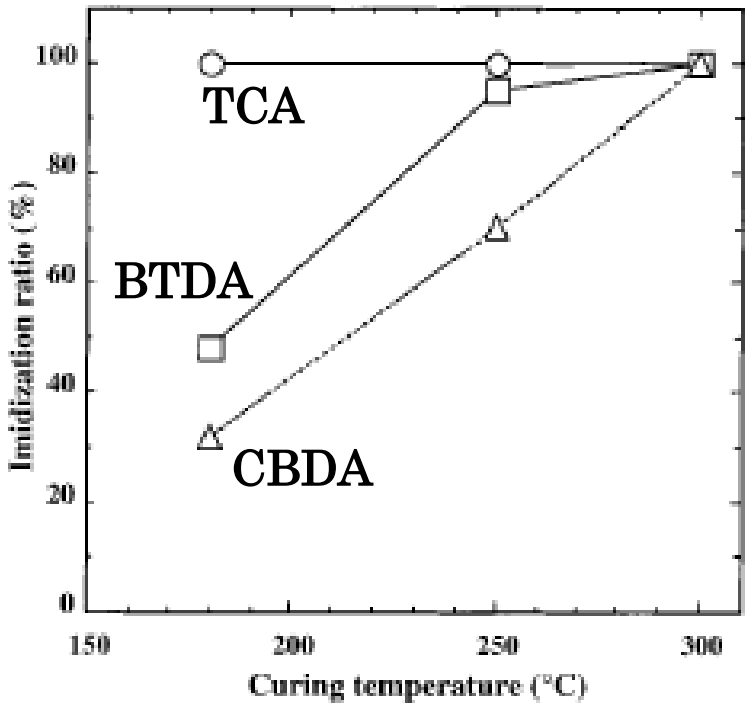

Fig. 3.1 Imidization ratio of PIs vs curing temperature [1]

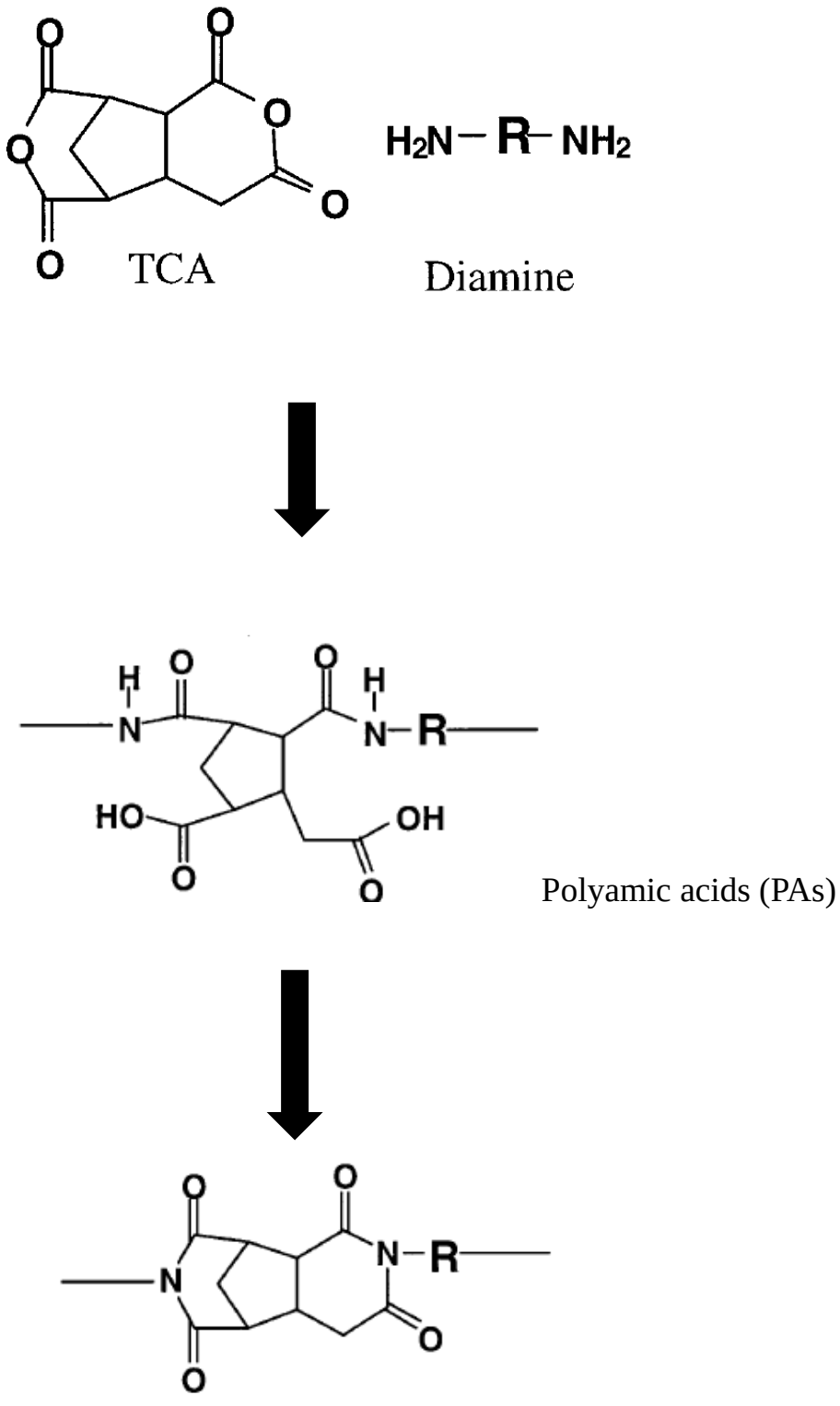

Fig. 3.2 Synthesis of soluble PI from TCA [2]

In order to do synthesis of soluble PI, Nishikawa [2] used alicyclic tetra carboxylic dianhydride (TCA) and diamine (4,4'-diaminediphenylmethane) for the precursor of polyamic acids (PAs). Then, the soluble PI is obtained through the catalysts of Py (pyridine) and Ac_2O (acetic anhydride) as shown in figure 3.2. For comparing the imidization ratio with other conventional PI , he also synthesized soluble PI from 3,3,4,4-benzophenone tetra carboxylic acid dianhydride (BTDA) and cyclobutane tetra carboxylic acid dianhydride (CBDA). Imidization ratio is calculated by taking the ratio between the peak strength of the imido-carbonyl groups and the benzene groups in Fourier transform infrared (FTIR) spectra. The imidization ratio of soluble PI from TCA attains the value of 100%, when the curing temperature is 180^{o}C, whereas the imidization ratio of conventional PI from BTDA and CBDA are about 50 % and 30%, respectively, at the curing temperature 180^{o}C. These are shown in figure 3.1. Therefore, the precursor of PAs from TCA (figure 3.2) is better candidate material for producing the soluble PI such that the higher imidization ratio is obtained.

Figure 3.3 shows the variation of the dichroic ratio of the LC cell with respect to the imidization ratio of PIs cured at 180^{o}C. This result indicates that they have a proportional relation and higher dichroic ratio corresponding to the better LC alignment. In this observation, the soluble PI from the precursor of PAs with TCA gives higher dichroic ratio compared to the soluble PI from the precursor of PAs with BTDA and with CBDA, because the precursor of PAs with TCA has the value of imidization ratio 100% at the curing temperature of 180^{o}C. Thus, the imidization ratio of the PI greatly affect the alignment of the LC. From the consideration of curing temperature, imidization ratio and dichroic ratio, the soluble of PI from the precursor

of PAs with TCA is a good candidate alignment film for controlling of LC molecule in LCDs performance.

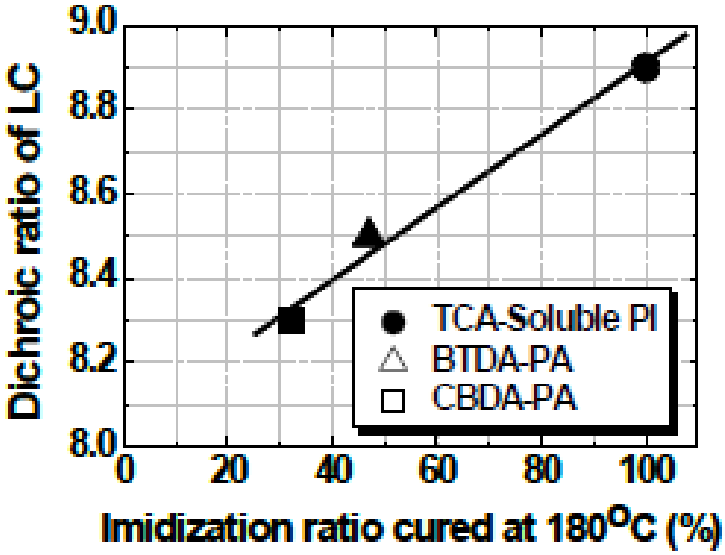

Fig.3.3 Dichroic ratio of LC vs imidization ratio of PI [3]

3.2 Stability of pretilt angle and electrical properties of novel alignment film

The rubbing strength on the polymer film is given by [4]

$$R_s = \gamma L \tag{3.1}$$

where γ is a coefficient, and it is related with the rubbing pressure, the fiber density of the rubbing cloth, the coefficient of friction etc. L is the total length of the rubbing cloth and it is expressed as

$$L = Nl(1 + \frac{2\pi nr}{v}) \quad (3.2)$$

where N is the number of rubbings, l is the contact length of the rubbing roller and the substrate, n is the number of rotations per second of the roller, v is the speed of movement of the substrate stage, and r is the radius of the roller as shown in figure 3.4(a). A rotating roller is covered by a cloth whose surface is made of short fibers, and a uniaxially movable platform to hold the substrate. In equation (3.2), l increases with rubbing pressure as controlled by the gap between the roller and the substrate. The terms, l are associated with stage force, roller down force and friction force. I would like to mention that there are two important mechanism occurs in the rubbing process: (i) microscopic grooves are generated in the polyimide layer during the elastic energy by the deformation of the polymer films and (ii) electrical charges produced when rubbing stress (rubbing pressure) is applied, which is say the piezoelectric effect. This effect is formed the static electric field between the polymer film and roller. However, the detail of mechanism has not yet been known.

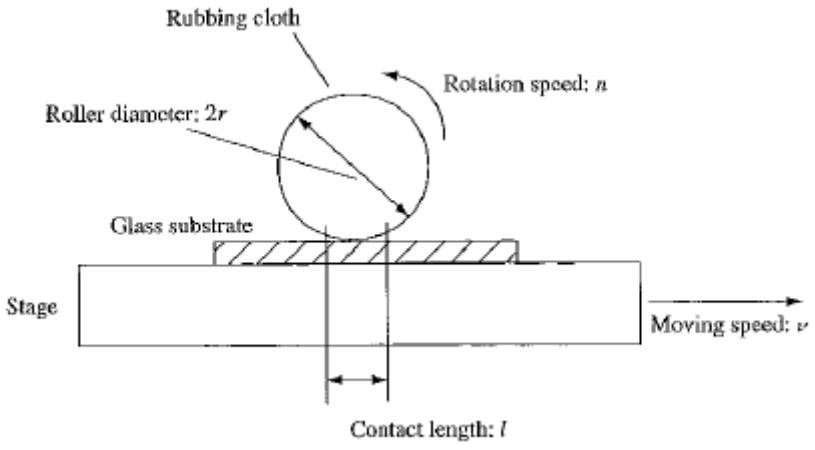

Fig.3.4 (a) Rubbing parameters [4]

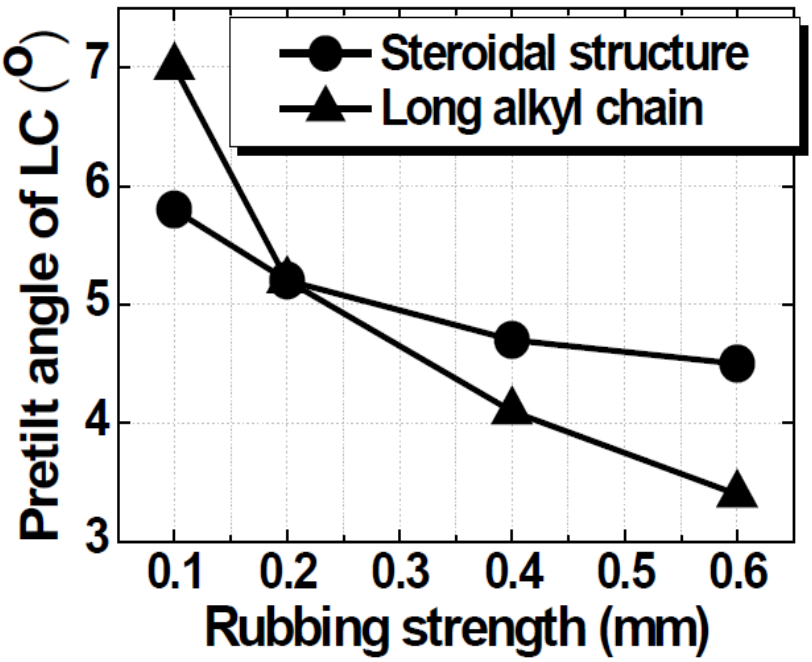

Fig.3.4 (b) Variation of the pretilt angle with the rubbing strength

According to consideration of the soluble PI with TCA, Nishikawa developed the novel diamines having a side chain with the steroidal structure in the soluble PI. Figure 3.4(b) shows the variation of the pretilt angle with respect to the rubbing strength. In this result, the variation of the pretilt angle (about 3^{o} with the rubbing strength from 0.1 to 0.6 mm) for a long alkyl chain structure is higher than that of the steroidal structure side chain (about 1.5^{o} with the rubbing strength of 0.1 to 0.6 mm). This indicates that the steroidal structure gives more stable pretilt angle compared to a long alkyl chain structure result.

Generation method of pretilt angle	Properties of LCDs		
	Controllable range of pretilt angle	Stability of pretilt angle	Electrical properties*
Addition of alkyl-containing compound to PI	3 - 5°	△	×
Introduction of alkyl chain into PI end position	3 - 10°	△	△
Introduction of alkyl chain into PI side position	3 - 90°	×	△
Introduction of alkyl chain into PI main chain	3 - 5°	△	△
Introduction of fluorine atoms into PI	3 - 40°	△	×
Target to realize LCD-TV	3 - 90°	○	○

○: Good, △: Fair, ×: Poor

Fig.3.5 Comparison of PI for different side chains with respect to range of the pretilt angle, the stability of the pretilt angle and electrical properties

The use of liquid crystal (LC) materials in LCDs are based on the following properties such as high electrical resistivity, large dielectric anisotropy, good chemical and thermal stability. Among them, high electrical resistivity are very much important due to the voltage holding ratio (VHR) characteristics. This characteristics is maintained by the voltages in the LC layer, which is kept during the selected period.

The voltage holding ratio (VHR) is given as follow [5]

$$\text{VHR (\%)} = \frac{V_t}{V_i} \times 100\% \tag{3.3}$$

where V_i is the initial or input pulse voltage, and V_t is the terminal voltage of the LC cell during the frame time.

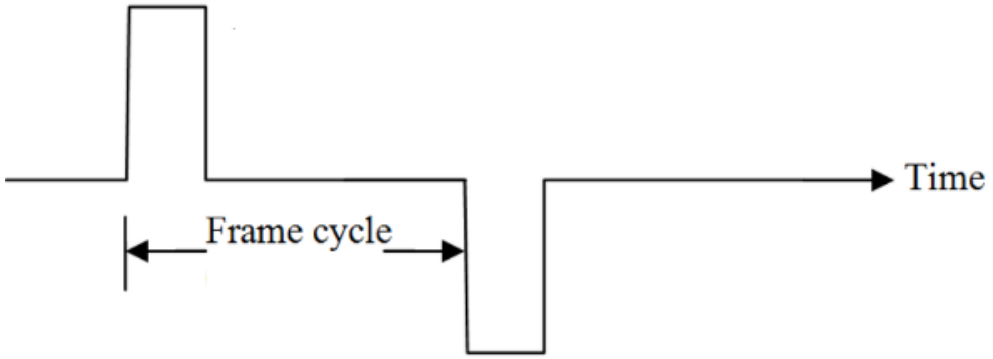

(a)

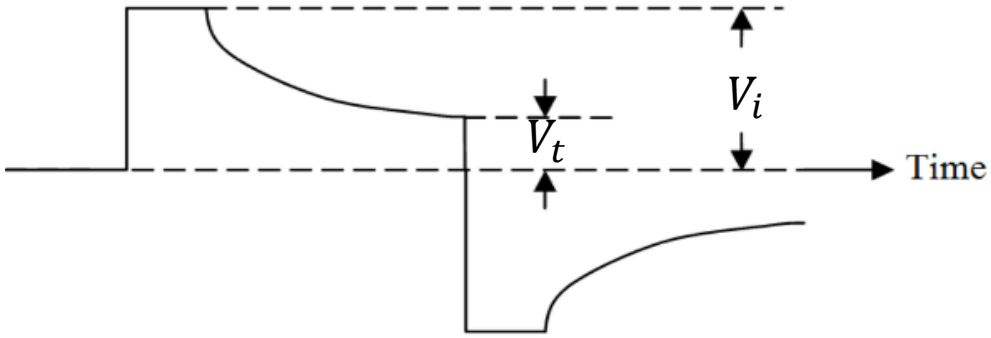

(b)

Fig. 3.6 (a) Schematic waveform applied to liquid crystal (b) Characteristics of the voltage holding ratio (VHR).

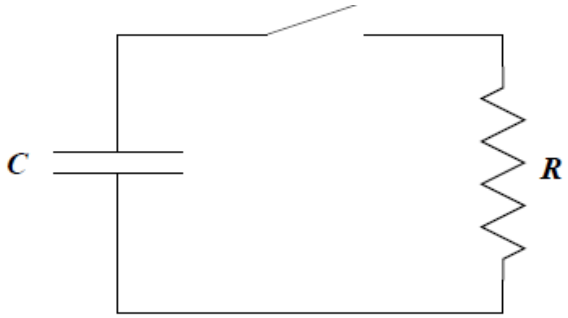

Fig. 3.7 Equivalent circuit

The decay of the voltage during the LC layer can be discussed with the assumption of discharge process through an equivalent circuit of resistance (R) and capacitor (C). Using the Kirchhoff's laws from figure 3.7, I can write,

$$\frac{q}{C} + RI = 0$$

$$\text{or, } \frac{q}{C} + R\frac{dq}{dt} = 0$$

$$\text{or, } \frac{dq}{q} + \frac{dt}{RC} = 0$$

$$\text{or, } \quad \frac{dq}{q} = -\frac{dt}{RC} \qquad (3.4)$$

Integrating the equation (3.4) and using the boundary condition $q = q_o$ at $t = 0$ and $q = q(t)$ at $t = t$, I get,

$$q(t) = q_o \exp(-\frac{t}{RC}) \qquad (3.5)$$

Therefore, the charge decays exponentially. The unit of the product RC is second. In analogy with the equation (3.5), the decay of the voltage for the liquid crystal is given by

$$V_t = V_i \exp(-\frac{t}{RC}) \qquad (3.6)$$

$$\text{or} \quad V_t = V_i \exp(-\frac{t}{\varepsilon\rho}) \qquad (3.7)$$

where R, C, ε and ρ are the resistance, the capacitance, the dielectric constant and the resistivity of liquid crystals, respectively.

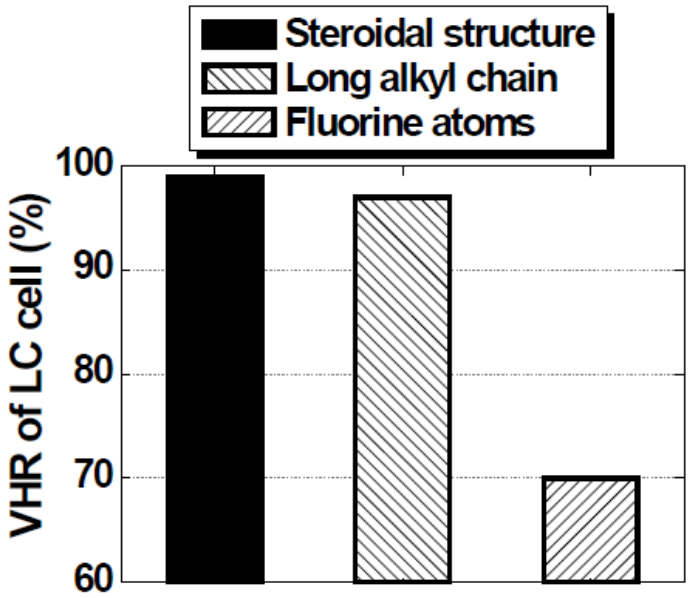

Fig. 3.8 Comparison of voltage holding ratio using different types of soluble PI

In order to reduce the flicker and image sticking of LCD, it is necessary to increase the parameter VHR i.e. higher voltage holding ratio giving good electrical properties. The voltage holding ratio's for three different types of soluble PI are shown in figure 3.8. In these results, a novel PI with steroidal structure side chain gives higher voltage holding ratio compared to other long alkyl chain and fluorine atoms.

From the consideration of stability of pretilt angle and voltage holding ratio, the soluble of PI with a steroidal structure side chain is a promising candidate alignment film in LCDs performance. Therefore, the soluble PI with steroidal structure of side chain is leading materials due to the advantages of a curing temperature, imidization ratio, dichroic ratio, stability of pretilt angle and voltage holding ratio in LCDs device performances and future improvement.

3.3 Surface enhanced Raman scattering spectrum (SERS)

Jason *et. al*. studied the molecular orientation of an aromatic polyimide containing cyanobiphenyl side chains [6] by using surface enhanced Raman scattering spectrum (SERS). This alignment surface containing pendent cyanobiphenyl mesogens was synthesized via a polycondensation of 2, 2' –bis (3-4-dicarboxi-phenyl) hexafluoropropane dianhydride (6FDA) with bis {ω-[4-(4-cyanophenyl) phenoxy] hexyl} 4,4'-diamino-2,2'-biphenyldicarboxylate (nCBBP, n=6), abbreviated as 6FDA-6CBBP, which is shown in figure 3.9.

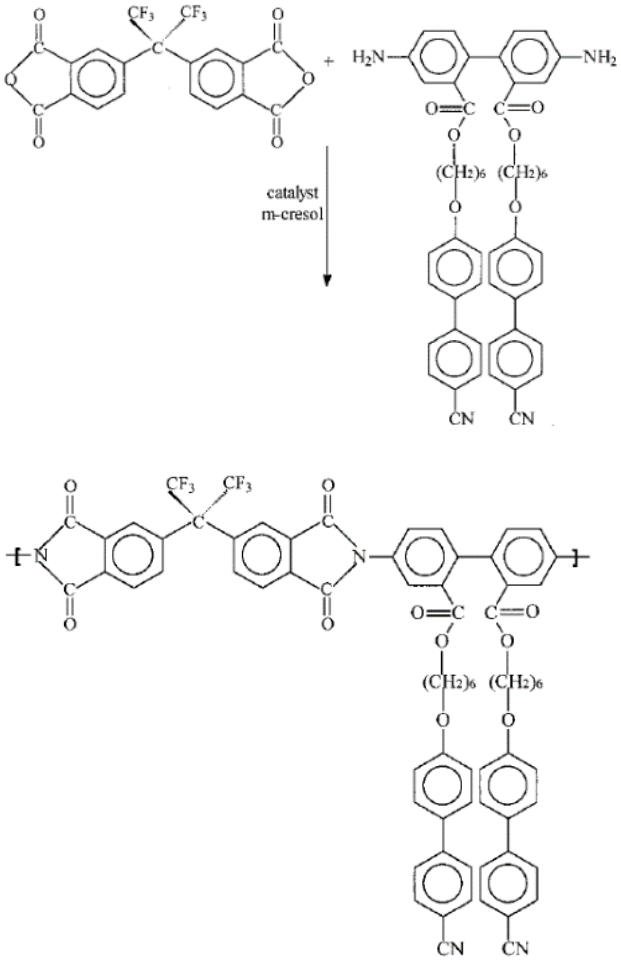

Fig.3.9 Synthesis of 6FDA-6CBBP

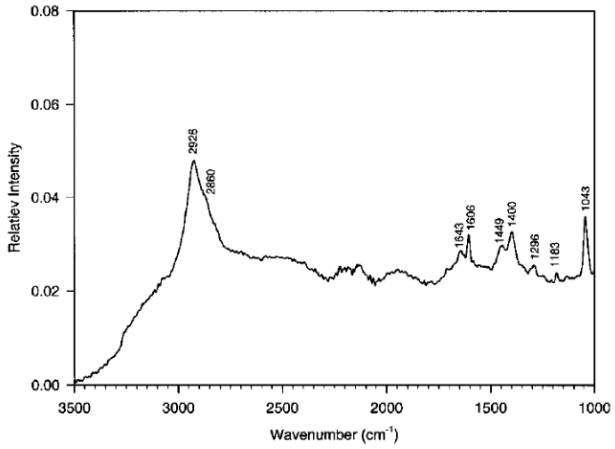

Fig.3.10 SERS spectrum of 6FDA-6CBBP from unrubbed thin film surface

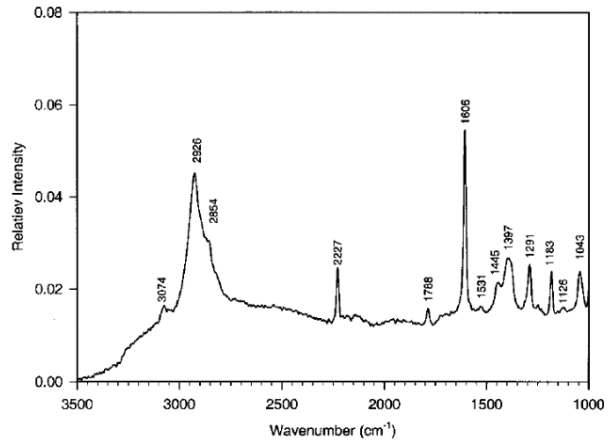

Fig.3.11 SERS spectrum of 6FDA-6CBBP from rubbed thin film surface

The band at 1606 cm^{-1} in figure 3.11 indicates the aromatic tangential ring stretching from the cyanobiphenyls. This is substantially enhanced at 2227 cm^{-1} due to the aromatic-cyano stretching. These two peaks were not observed in the unrubbed film surface as shown in figure 3.10. It is confirmed that the cyanobiphenyls adopt a tilted angle with respect to the rubbing. Therefore, the rubbing treatment is very much important for adjusting the molecular orientation of the polymer side chain.

3.4 Atomic force microscopy (AFM) results

Huang *et al*. studied the rubbing induced molecular alignment on an orienting layer of polyimide with and without alkyl side chains [7]. In this study, they mentioned the polymer film with alkyl branch (AL-3046) and without alkyl branch (AL-1254). The phase retardation observation indicates that the molecular anisotropy introduced into the rubbed AL-1254 layer saturates after three repetition of rubbing (as shown in figure 3.12). On the other hand, the phase retardation investigation indicates the molecular anisotropy introduced into the rubbed AL-3046 layer saturates after two repetition of rubbing (as shown in figure 3.13).

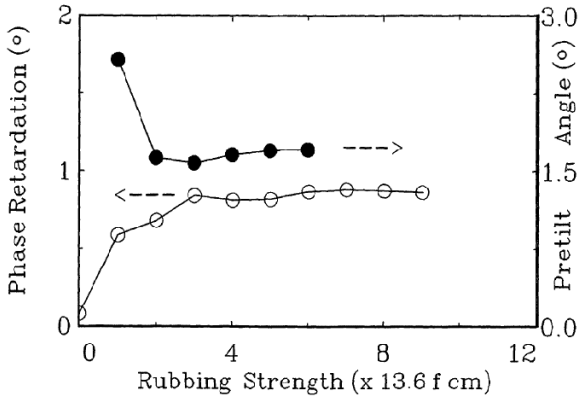

Fig. 3.12 AL-1254

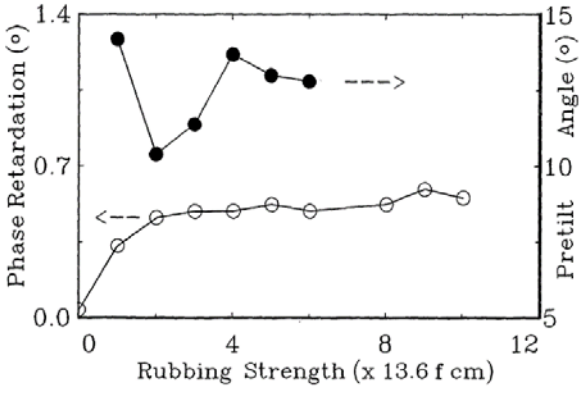

Fig. 3.13 AL-3046

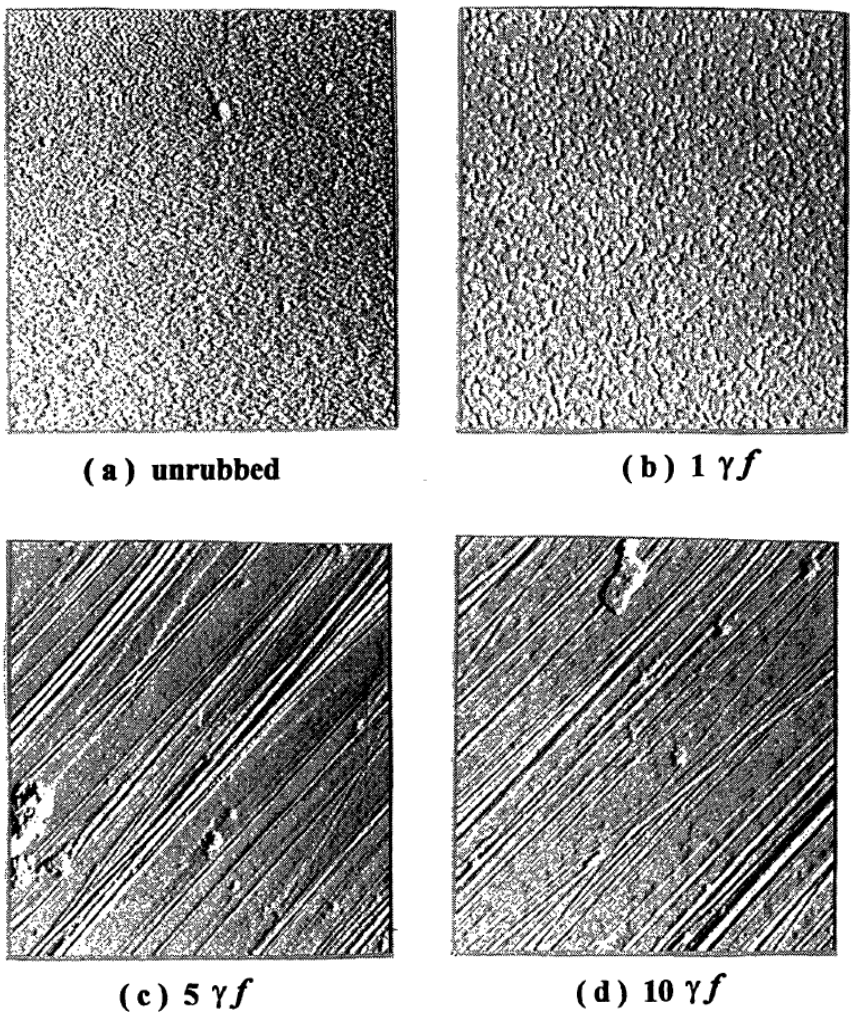

Fig.3.14. Topographic images of (a) an unrubbed AL-3046 polyimide film, and rubbed films with strength (b) $R_s = 1\gamma f$ (c) $R_s = 5\gamma f$ and (d) $R_s = 10\gamma f$, The scan area of the images is $20\mu m \times 20\mu m$, f is the characteristic coefficient of the interface between the rubbing cloth and the substrate.

Figure 3.14 shows the topographic images of rubbed AL-3046 films with different rubbing strengths, R_s. Both of the surfaces of an unrubbed AL-3046 film and a film with a rubbing strength of 13.6f cm do not show any observable rubbing scars. The fine features in the surface morphology disappeared as the rubbing strength exceed $R_s = 5\gamma f$. The rubbing scars were clearly observed in 3.14(c) to 3.14(d).

3.5 Surface orientation study by second harmonic generation (SHG)

Shirota *et al*. studied the orientational distribution of the side chains of polyimide films for liquid crystal alignment [8]. The chemical structure of the polyimide, 4CF3-PI is shown in figure 3.15.

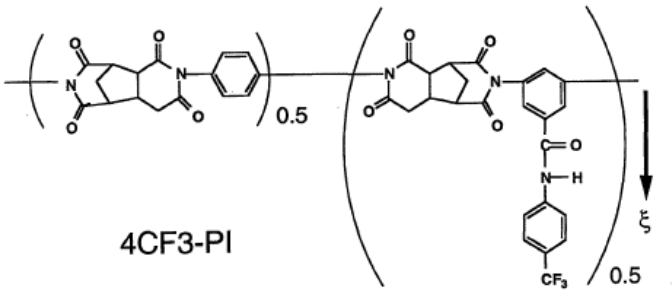

Fig. 3.15 The polyimide has trifluorocarbon group at the terminal benzene attached to the amide bond. ξ is the predominant direction responsible for molecular susceptibility.

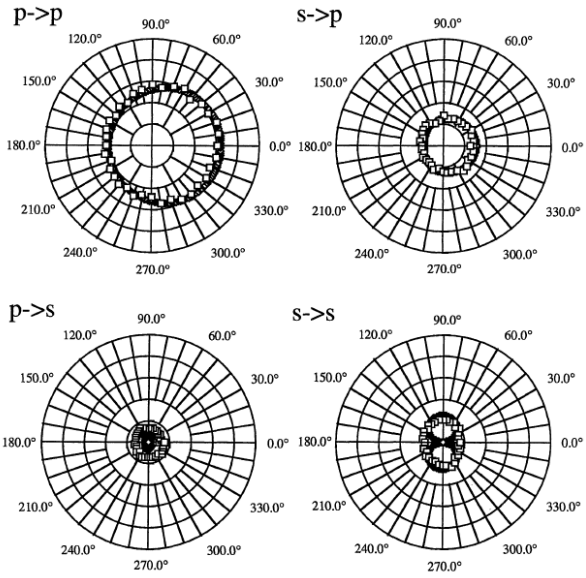

Fig. 3.16 Optical second harmonic result from rubbed 4CF3-PI

In that study, the molecular orientation of the polyimide side chain was determined from optical SHG measurement results as shown in figure 3.16. The symmetry of the polymer side chain was changed from C_∞ to C_s by the rubbing treatment. They determined $\chi^{(2)}$ elements of the polymer side chains towards rubbing direction considering only real values of $\chi_{ijk}^{(2)}$ elements as follows: $\chi_{zzz}^{(2)}$ = 1.00 , $\chi_{xxx}^{(2)}$ =-0.32, $\chi_{zyy}^{(2)}$ =0.63, $\chi_{zxx}^{(2)}$ = 0.65 , $\chi_{zxz}^{(2)}$ = - 0.03, and $\chi_{xyy}^{(2)}$ = -0.09, where x is in the rubbing direction and z is in the direction normal to the film surface. The values of $\chi_{\mathrm{ijk}}^{(2)}$ are normalized by that of $\chi_{\mathrm{zzz}}^{(2)}$. There is lack of accuracy here because the analysis considered only the real values of $\chi_{ijk}^{(2)}$ elements. I suggest, it is necessary to consider the values of $\chi_{ijk}^{(2)}$ elements in the complex plane.

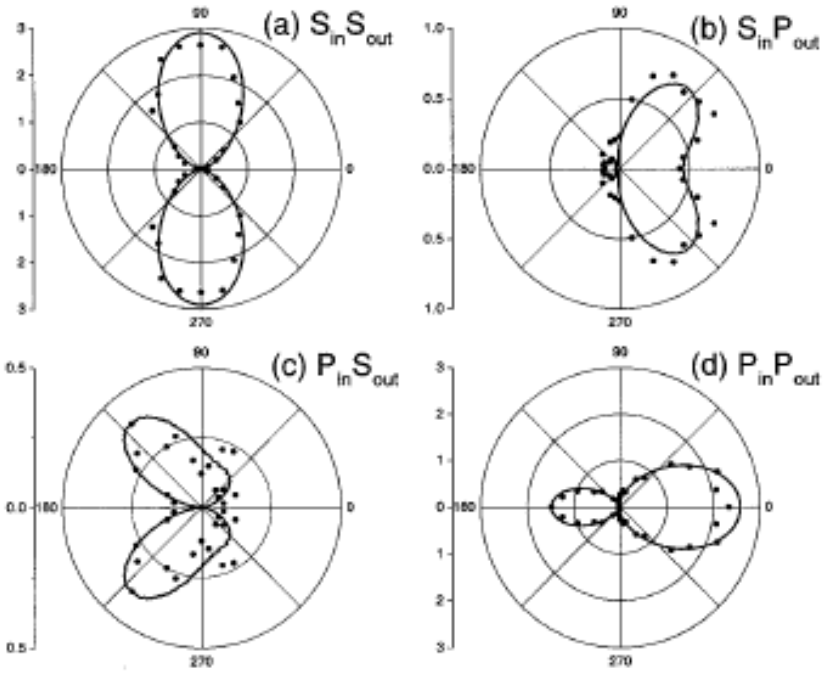

Fig. 3.17 Optical second harmonic result of rubbed 6FDA-6CBBP.

On the other hand, Jason *et al.* also studied the molecular orientation of an alignment surface of an aromatic polyimide containing cyanobiphenyl side chains [6] by using surface second harmonic generation. Anisotropic SHG patterns of 6FDA-6CBBP are shown in figure 3.17. They determined six independent nonvanishing elements of $\chi_{ijk}^{(2)}$ as follows: $\chi_{zzz}^{(2)} = -0.041$, $\chi_{xxx}^{(2)}$ =-1.0, $\chi_{zyy}^{(2)}$ =-0.072, $\chi_{zxx}^{(2)}$ = -0.12, $\chi_{zxz}^{(2)}$ = - 0.031, and $\chi_{xyy}^{(2)}$ = 0.22. The values of $\chi_{\mathrm{ijk}}^{(2)}$ are normalized by that of $\chi_{\mathrm{xxx}}^{(2)}$. In this analysis, they also considered only real values of $\chi_{ijk}^{(2)}$ elements for the determination of the tilt angle of the polymer side chain toward the rubbing direction.

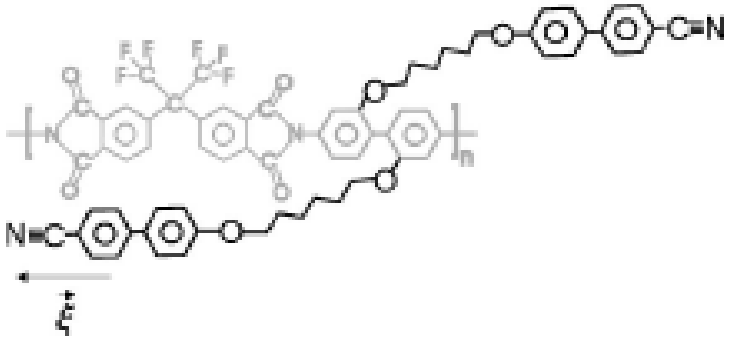

Fig. 3.18 Chemical structure of 6FDA-6CBO

Fig. 3.19 Chemical structure of 5CB

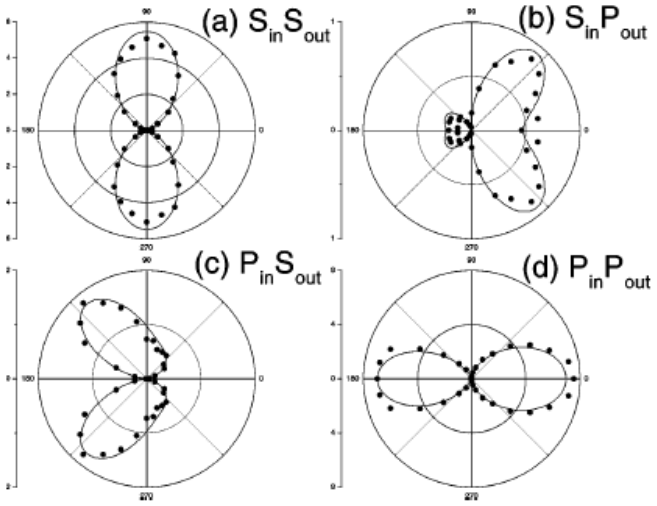

Fig. 3.20 Optical second harmonic patterns of rubbed 6FDA-6CBO surface ($\chi^{(2)}_{CBO}$)

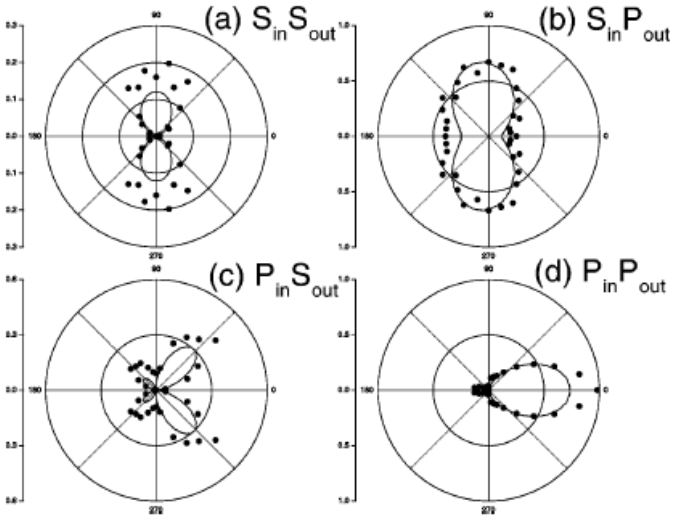

Fig. 3.21 Optical second harmonic patterns for 5CB monolayer on rubbed 6FDA-6CBO $\chi^{(2)}_{eff}$

Hong *et al*. studied the orientation of side chains of rubbed polyimide surface by using second harmonic generation (SHG) [9]. In this study, they observed SHG from a rubbed 6FDA-6CBO surface shown in figure 3.20. They also measured SHG for a

5CB monolayer on rubbed 6FDA-6CBO as shown in figure 3.21. The effective nonlinear second order nonlinear susceptibility is given by:

$$\chi_{eff}^{(2)} = |\chi_{CBO}^{(2)} + \chi_{5CB}^{(2)}\exp(i\varphi)| \quad (3.9)$$

where $\chi_{CBO}^{(2)}$ belongs to the bare 6FDA-6CBO surface, φ is the relative phase between $\chi_{CBO}^{(2)}$ and $\chi_{5CB}^{(2)}$. The fitting results of figure 3.20 were done with the six independent nonvanishing $\chi_{(CBO)ijk}^{(2)}$ components as follows $\chi_{zzz}^{(2)} = -0.020$, $\chi_{xxx}^{(2)}$ =-1.0, $\chi_{zyy}^{(2)}$ =-0.020, $\chi_{zxx}^{(2)}$ = -0.076, $\chi_{zxz}^{(2)}$ = 0.036, and $\chi_{xyy}^{(2)}$ = 0.23. The values of $\chi_{\mathrm{ijk}}^{(2)}$ were normalized by that of $\chi_{\mathrm{xxx}}^{(2)}$. In this analysis, they considered only real values of $\chi_{ijk}^{(2)}$ elements for the calculation of the molecular orientation of the polymer side chain. They also evaluated the fitting result of figure 3.21 as follows: $\chi_{zzz}^{(2)}$ = 0.041, $\chi_{xxx}^{(2)}$ =--0.81, $\chi_{zyy}^{(2)}$ =0.101, $\chi_{zxx}^{(2)}$ = 0.23, $\chi_{zxz}^{(2)}$ = - 0.028, and $\chi_{xyy}^{(2)}$ = -0.91. In here, they also considered only real values $\chi_{ijk}^{(2)}$ components for the investigation of orientational distribution of 6CBO side chains on a rubbed 6FDA-6CBO surface and 5CB molecules adsorbed on the surface.

In summary, I have reviewed the study of SHG of soluble PI films as shown in figure 3.22. The number of SHG works of polyimide is not big enough. In this regard, research work on polyimide alignment thin film by optical SHG for improving the performances of LCDs device needs a development. On the other hand, most of reports have considered only the real values of $\chi_{ijk}^{(2)}$ component, which has less accuracy for

determining tilt angle of the polymer chain toward the rubbing direction, because $\chi_{ijk}^{(2)}$ is a complex value. In order to improve the analysis method, it is necessary to analyze $\chi_{ijk}^{(2)}$ components in the complex plane. I have also studied a novel soluble polyimide (PI) with a steroidal structure side chain. It has many advantages such as stability of pretilt angle, controllable range of pretilt angle (3-90^{o}) and good electrical properties (higher voltage holding ratio). So far as I know, no optical second harmonic generation (SHG) measurement for such type of PI has been reported. Therefore, this is the first report about the orientational distribution of rubbed polyimide (PI) with a steroidal structure side chain studied by SHG. In this research, in order to obtain the tilt angle of the polymer side chain toward the rubbing direction, I did consider the $\chi_{ijk}^{(2)}$ components in the complex plane for higher accuracy. Therefore, this is the first report for the molecular orientation of such kind of rubbed polyimide (PI) with a steroidal structure side chain in my thesis by using the $\chi_{ijk}^{(2)}$ components in the complex plane.

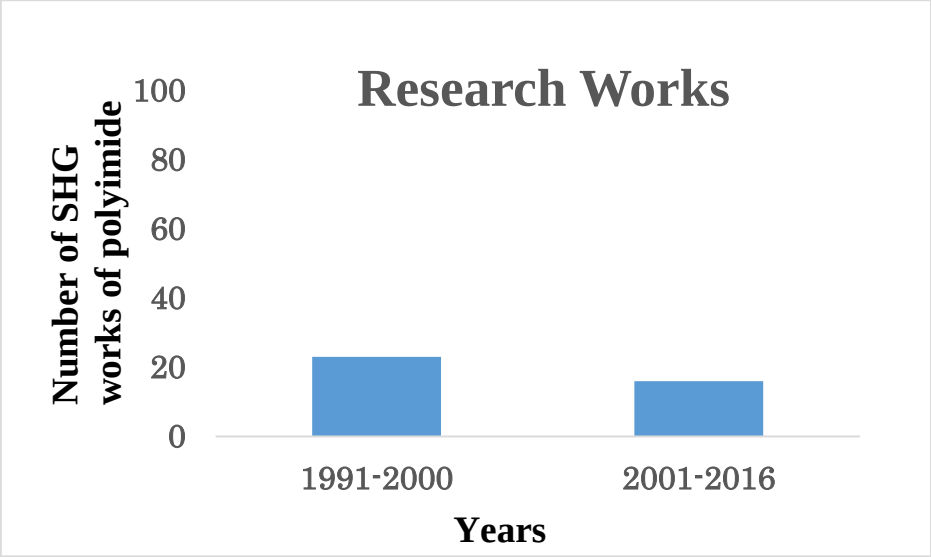

Fig. 3.22 Research study of polyimide

References:

[1] M. Nishikawa, Polym. Adv. Technol. 11, 404 (2000)

[2] M. Nishikawa, Y. Matsuki, N. Bessho, Y. Imura and S. Kobayashi J. Photopolym. Sci. Technol., 8(2), (1995)

[3] M. Nishikawa, J. Photopolym. Sci. Technol., 24(3), (2011)

[4] K. Takatoh, M. Hasegawa, M. Koden, N. Itoh, R. Hasegawa , M. Sakamoto, Taylor & Francis, New York (2005)

[5] M. Oh-E et al, Jpn. J. Appl. Phys. 36, (8A) (1997)

[6] J. J. Ge, C. Y. Li, G. Xue, I. K. Mann, D. Zhang, S. Y. Wang, F. W. Harris, S. Z. D. Cheng, S. C. Hong, X. Zhuang, and Y. R. Shen, J. Am. Chem. Soc. 123, 5768, (2001)

[7] J. Y. Huang, J. S. Li, Y. S. Juang and S. H. Chen, Jpn. J. Appl. Phys. 34, Pt. 1, No. 6A, 3163 (1995)

[8] K. Shirota, K. Ishikawa, H. Takezoe, A. Fukuda and T. Shibashi, Jpn. J. Appl. Phys. 34, Pt. 2, No. 3A, L316 (1995)

[9] S.C. Hong, M. Oh-e, X. Zhuang ,Y. R. Shen, J. J. Ge, F. W. Harris and S. Z. D. Cheng, Phys. Rev. E 63**,** 051706 (2001)

Chapter 4

Materials and Nonlinear Optical Experiment

4.1 Synthesis of polyamic acid (PAA) solution

All source materials were used as received without further purification. A 500 ml round flask was charged with 1, 4-Phenylenediamine (10.30 g, 95.2 mmol), side-chain diamine (40.8 mmol) and 240 g of NMP (N-methylpyrrolidone) under the nitrogen atmosphere. After 1 hour stirring, 2, 3, 5-tricarboxycyclopentyl acetic dianhydride (23.36 g, 126.5 mmol) was added to the solution and stirred at 25ºC for 3 hours. The solution was diluted to 3.5 wt% with NMP and ethylene glycol monobutyl ether and filtered through a 0.20 μm Teflon filter.

4.2 Preparation of polyimide (PI) film

The PAA solution was spin-coated onto an ITO-coated glass substrate, and then the coated substrate was dried at 80 °C for 2 min to remove the solvent. The thickness was controlled by spinning rate. The pre-dried film was annealed in an oven at 230º C for 30 minutes under nitrogen atmosphere to obtain PI film of 100 nm. The PI films were rubbed by a rubbing machine using nylon cloth.

Scheme 1. Synthesis of PAA

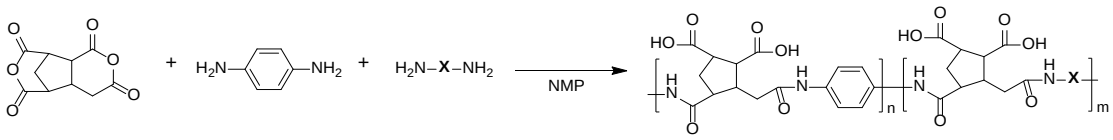

Scheme 2. Synthesis of PI

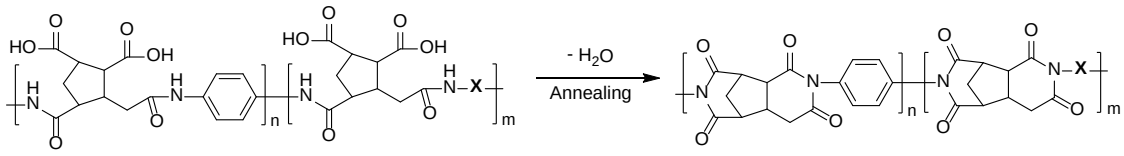

Scheme 3. Side-chain diamines (H_2N-**X**-NH_2)

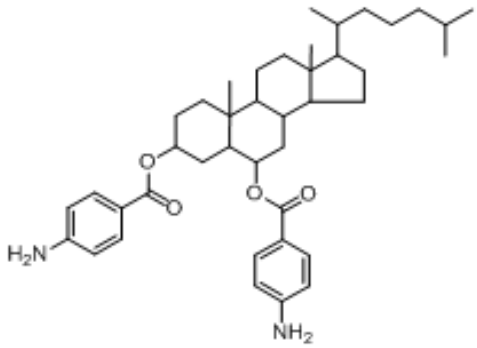

Side-chain diamine A (PAA-1)

Scheme 4. Synthesis of side-chain diamine A

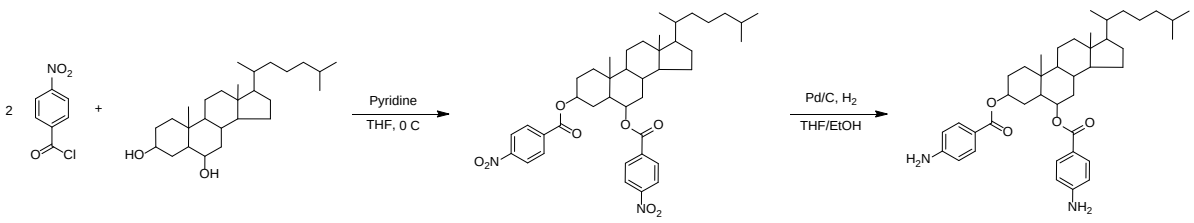

Fig.4.1 Synthesis of the novel PI film with side chain

4.3 Spin coating of polymer films

Spin coating is largely used for the fabrication of thin film coatings over wide areas with high structural uniformity. Research in the scope of spin coating has been extended in the recent years [1]. Spin coating is the process in which to apply a solution into a horizontal rotating disc, resulting in ejection and evaporation of the solvent, and leaving a liquid or solid film. It is a unique technique in order to get a planner substrate over a large area ($A \geq 30$ cm) with a highly controllable and reproducible film thickness. The schematic spin coating process is shown in figure 4.2. This technique is applied to both organic, inorganic, and inorganic/organic solution mixtures.

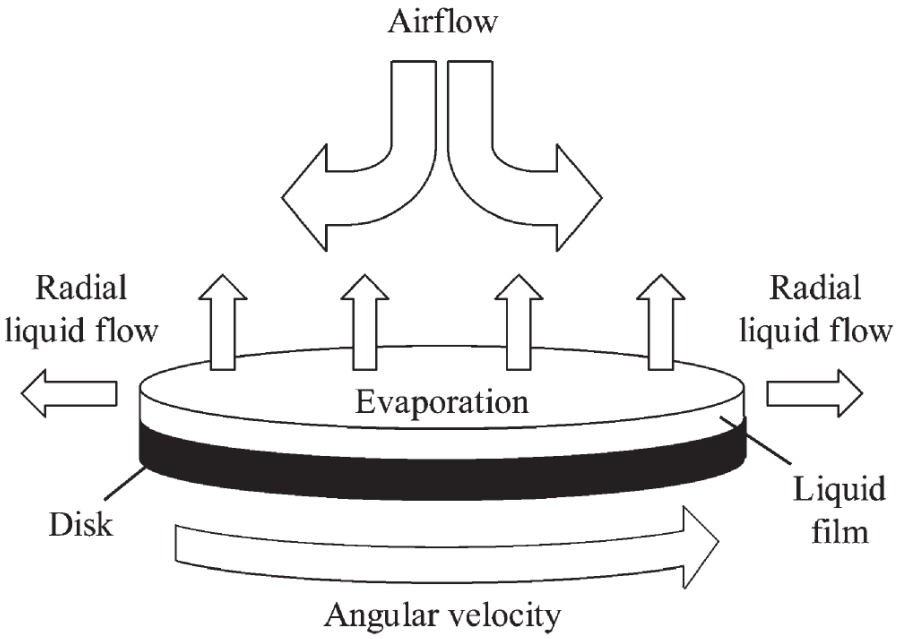

Fig.4.2 Spin coating process.

The most effective use of the spin-coating method is for microelectronics applications [2]. The important factors in spin coating process is the spin speed. The disk should be either static or rotating with lower angular velocity in the deposition time. After that, the disc is rapidly accelerated to get high spin speed. The adhesive force and centrifugal force are acting on the rotating liquid, which causes flow of liquid in the radial direction. Finally the solvent is evaporated, and a uniform solid polymer film is produced.

4.4 Rubbing treatment

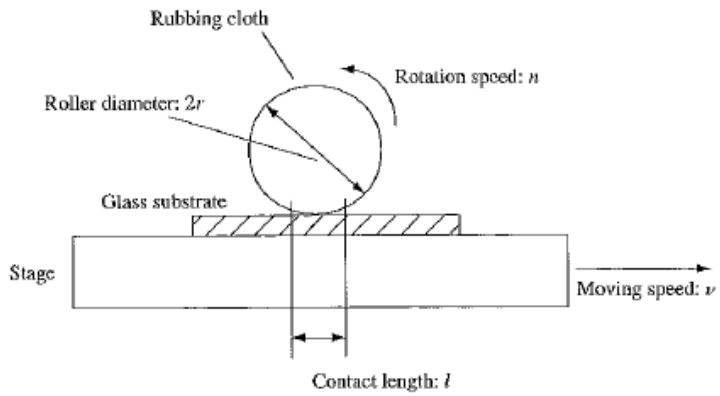

Fig. 4.3. Rubbing process

The PI film was rubbed by a rubbing machine using nylon cloth. In the mechanical rubbing process, the rotational speed of the roller was 400 rpm, the translational speed was 30 mm/sec, and the pile impression depth indicating the rubbing strength was 0.4 mm. The film was rubbed only one time. The SHG study of the dependence of the θ_{ave} (average tilt angle) on the rotational speed of the rubbing roller and rubbing strength is a future topic. I anticipate that θ_{ave} will not strongly depend on these parameters

because the steroidal structure is very stable, and from my experience [3] the pretilt angle of the liquid crystal molecules depend rather on the content of the steroidal structure side chains than the rubbing strength or the rotational speed of the rubbing roller.

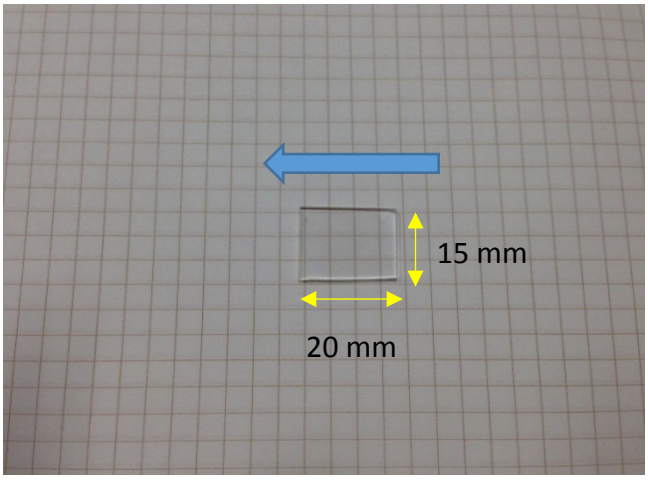

Fig.4.4 Rubbed novel PI film with diamine A steroidal side chain, blue arrow sign indicates the rubbing direction, the dimensions of the sample surface are 20 mm and 15 mm

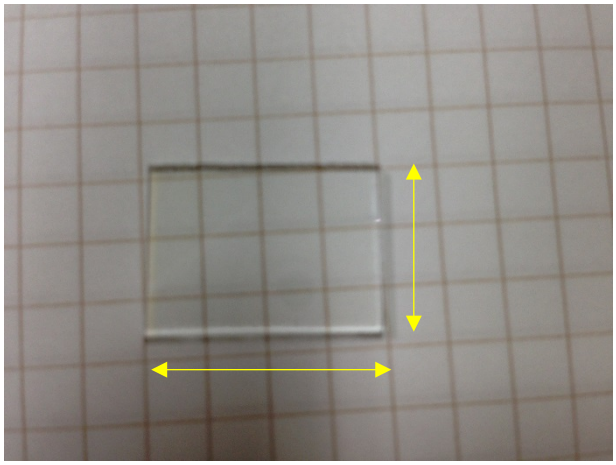

Fig.4.5 Unrubbed novel PI film with diamine A steroidal side chain, the area of the sample surface is 20×15 mm^2

4.5 Optical second harmonic generation experiment

The optical setup of SHG measurement is shown in Fig. 4.8. I used the fundamental light of Nd: YAG laser with photon energy of 2.33eV with a pulse duration of 30 ps and a repetition rate of 10 Hz as the excitation light of SHG. The photon energy of 2.33 eV was chosen according to literature [4-6]. The bandgap of polyimide PI is 3.317 eV [7]. Normally, optical bandgap is determined from the intercepts of the plots of $(\alpha h\nu)^{1/2}$ versus $h\nu$ on $h\nu$ axis, where α is the optical absorption coefficient, h is the Planck's constant, and ν is the frequency of photon. The two photon energy $2\hbar\omega$ = 4.66 eV is sufficiently larger than 3.317 eV. That is why, I used 2.33 eV photon energy as a fundamental light.

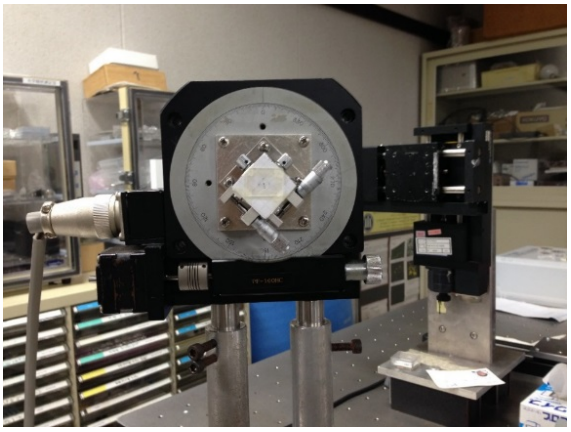

Fig.4.6 Rotational stage

The incident laser beam was directed onto the rubbed and unrubbed polyimide samples at 45^{o} from the surface normal. The sample was rotated from 0^{o} to 350^{o} with 10^{o} steps on the rotational stage as shown in figure 4.6. The fundamental beam was focused by a lens with a focal length of 350 mm. The beam was kept slightly off focus at the sample surface to avoid the sample damage.

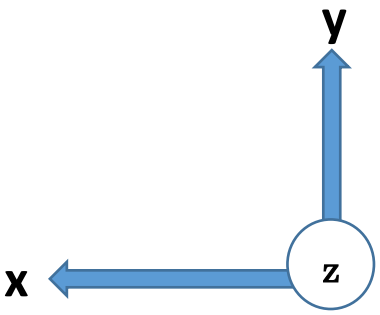

Fig. 4.7 Sample coordinate, x is in the rubbing direction, and z is the direction normal to the film surface.

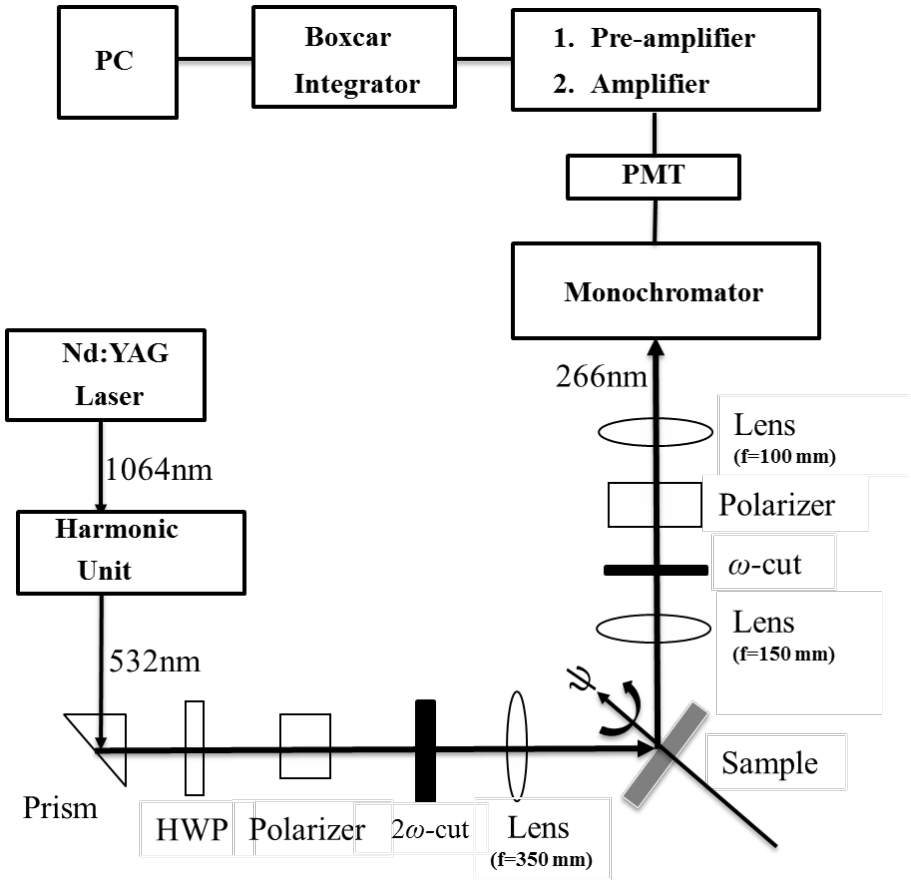

Fig. 4.8. Experimental optical schematic diagram for SHG measurement. PMT and HWP represent photomultiplier and half wave plate, respectively.

The second harmonic signal with the photon energy of 4.66 eV was detected from the sample. It was separated from the fundamental light with $\omega -$ cut filter put in the output path beam. Then it was detected by a monochromator and photomultiplier, converted to the electrical signal, amplified with a boxcar integrator and finally accumulated in a computer. I measured SHG generated from the sample with four combinations of input/output polarizations denoted as P_{in}/P_{out}, P_{in}/S_{out}, S_{in}/P_{out}, and S_{in}/S_{out}. Here, for example, the notation S_{in}/P_{out} means that the fundamental light is s-polarized and SHG light is p-polarized.

Table 4.1: Linear dielectric constants of the synthesized polyimide film after rubbing. ε' and ε" are the real and imaginary parts of the dielectric constants, respectively.

Photon energy	ε'	ε"
2.33eV	2.515	0.000
4.66eV	2.622	0.719

Table 4.2: Refractive index values at different wavelengths. Sample: side chain diamine A

		256 nm	532nm	999nm
Sample	before rubbing	1.599	1.592	1.555
	after rubbing 0 deg	1.587	1.586	1.551
	after rubbing 180 deg	1.588	1.586	1.557

References

[1] K. Norrman, A. G. Siahkali and N. B. Larsen, Annu. Rep. Prog. Chem., Sect. C, 101, 174 (2005)

[2] M. D. Tyona, Advan. Mats. Research, 2(4) 195 (2013)

[3] M. Nishikawa, J. Photopolym. Sci. Technol. 24(3), 317 (2011)

[4] T. Sakai, K. Ishikawa and H. Takezoe, Liquid Crystal 29(1), 47 (2002)

[5] T. Sakai, J. G. Yoo, Y. Kinoshita, K. Ishikawa, H. Takezoe, A. Fukuda, T. Nihira and H. Endo, Appl. Phys. Lett. 71(16), 2274 (1997)

[6] S.C. Hong, M. Oh-e, X. Zhuang and Y. R. Shen, Phys. Rev. E 63, 051706 (2001)

[7] F. H. Wang et al. Nanomaterials 6, 88 (2016)

Chapter 5

Results and Discussion

5.1 Optical second harmonic generation of unrubbed polyimide thin films with steroidal structure side chains diamine A

The second harmonic generation (SHG) intensities as a function of the rotational angle ψ of the unrubbed PI thin films with steroidal structure side chains with input/output polarization combinations are shown as black dots in figure 5.1. The solid thin curves are the theoretical fits, and the black dots are experimental results. The angle ψ is defined as zero when the incidence plane is parallel to one edge of the glass substrate. There was no anisotropy in the SHG patterns of Fig. 5.1 (a) to (d) of the unrubbed sample. The SHG of Sin/Sout and Pin/Sout are very weak. The symmetry of the polymer side chains belongs to C_∞. If the molecular distribution is polar with respect to the surface normal direction (z-direction), and isotropic in the surface (x-y) plane as in unrubbed polymer films, the patterns can be reproduced only by $\chi^{(2)}_{zxx}$, $\chi^{(2)}_{zyy}$, and $\chi^{(2)}_{zzz}$ elements. This is because the polymers are completely randomly oriented. There are nonvanishing nonlinear second order susceptibility components as in the followings.

$$\chi^{(2)}_{zzz} = N_s < \cos^3\theta > \beta^{(2)}_{\xi\xi\xi} \qquad (5.1)$$

$$\chi_{zii}^{(2)} = \chi_{iiz}^{(2)} = \chi_{izi}^{(2)} = (1/2)\mathrm{N_s} < sin^2\theta\cos\theta > \beta_{\xi\xi\xi}^{(2)} \quad (5.2)$$

where $\mathrm{N_s}$ is the molecular density of the surface, $\beta_{\xi\xi\xi}^{(2)}$ is the molecular susceptibility component along the molecular long axis ξ. θ is the polar angle between ξ and z-axis. The bracket sign indicates the average over molecular orientational distribution function.

The SHG intensity at frequency 2ω induced by nonlinear polarization is given by [1]

$$\mathrm{I_{2\omega}} \propto |\vec{\mathrm{P}}_{2\omega}^{2}|^2 \quad (5.3)$$

and

$$\vec{\mathrm{P}}_{2\omega}^{2} = \varepsilon_o \chi_{\mathrm{s,eff}}^{(2)} : \vec{\mathrm{E}}(\omega)\vec{\mathrm{E}}(\omega) \quad (5.4)$$

Here $\vec{\mathrm{E}}(\omega)$ is the incident electric field at frequency ω and $\chi_{\mathrm{s,eff}}^{(2)}$ is the effective second order surface nonlinear susceptibility tensor of the illuminated medium [2]. The susceptibility tensor $\chi_{\mathrm{s,,eff}}^{(2)}$ is defined as [3]

$$\chi_{\mathrm{s,eff}}^{(2)} = [\hat{\mathrm{e}}(2\omega).\mathrm{L}(2\omega)]\chi^{(2)} : [\mathrm{L}(\omega).\hat{\mathrm{e}}(\omega)][\mathrm{L}(\omega).\hat{\mathrm{e}}(\omega)] \quad (5.5)$$

where $\hat{\mathrm{e}}(2\omega)$ and $\hat{\mathrm{e}}(\omega)$ are the unit polarization vector for the second harmonic beam at frequency 2ω and fundamental beam at ω, respectively. $\mathrm{L}(2\omega)$ and $\mathrm{L}(\omega)$ are the local field factor or Fresnel factor tensors for SHG field and fundamental beam, respectively. The independent nonvanishing components can be determined by using SHG measurement. Therefore, the average polar angle can be

determined under the approximation of the distribution function. If one considers that the delta δ-function is the distribution function, then the relation obtained is as

$$\theta = tan^{-1}\left(\frac{2\chi^{(2)}_{zii}}{\chi^{(2)}_{zzz}}\right) \tag{5.6}$$

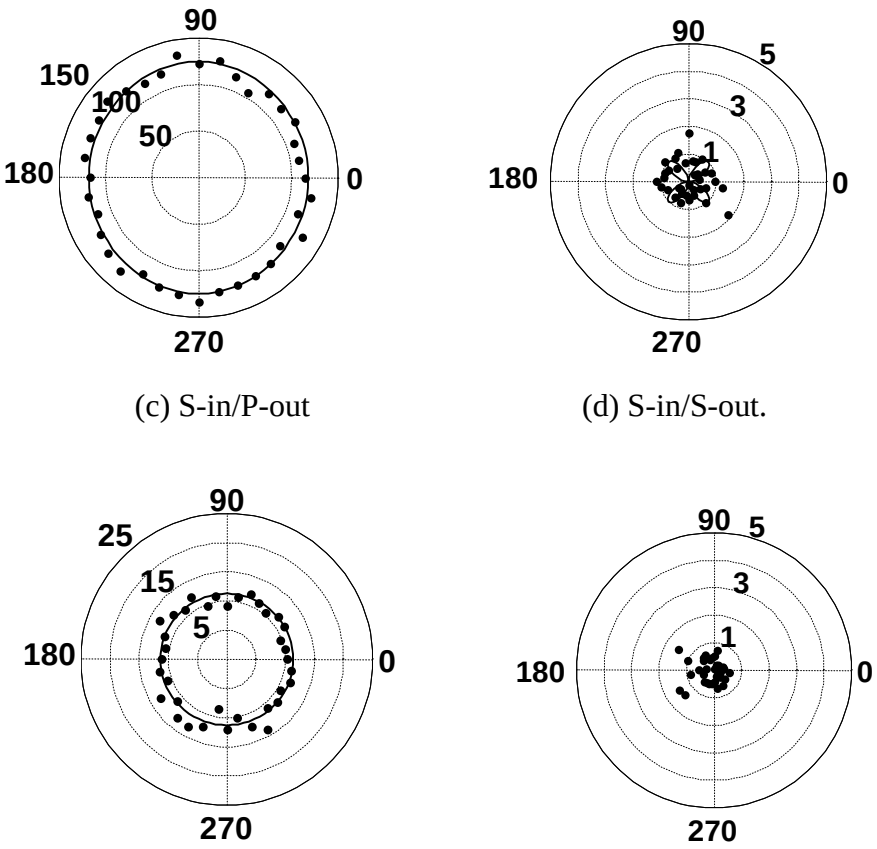

Fig. 5.1. Optical SHG signals from the unrubbed polyimide thin layer surface as a function of the sample rotational angle around its surface normal. The input-output polarization combinations are (a) P-in/P-out, (b) P-in/S-out, (c) S-in/P-out, and (d) S-in/S-out.

5.2 Optical second harmonic generation of rubbed polyimide thin films with steroidal structure side chains diamine A

The SHG intensity as a function of the rotational angle ψ of the rubbed PI thin films with steroidal structure side chains with input/output polarization combinations are shown as black dots in figure 5.2.

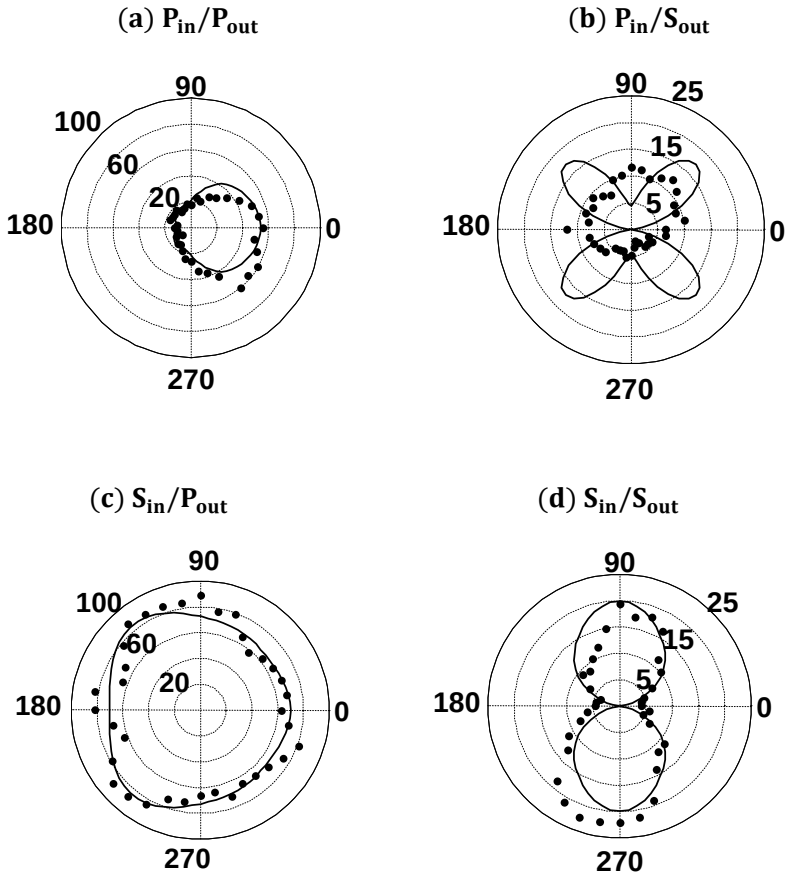

Fig. 5.2. Optical SHG results from the rubbed polyimide thin layer surface as a function of the sample rotational angle around its surface normal. The input-output polarization combination are (a) P-in/P-out, (b)P-in/S-out, (c) S-in/P-out, and (d) S-in/S-out. The solid thin curves are the theoretical fits, and the black dots are experimental results.

Here ψ is defined as zero when the wave vector component of the fundamental beam parallel to the film face is in the same direction as that of the rubbing. The radial length indicates the SHG intensity. The characteristic anisotropic patterns are observed due to the rubbing for all the polarization combinations. Namely, the patterns from Figs. 5.2(a) to 5.2 (d) are mostly symmetric with respect to the horizontal line connecting the 0^o and 180^o angle marks. However, for P_{in}/P_{out} and S_{in}/S_{out} polarization combination, they are not symmetric with respect to the line connecting 90^o and 270^o angle marks. The curves in Fig. 5.2 are the theoretical fitting. In the P_{in}/P_{out} polarization combination, the SHG intensity is strong at $\psi = 0^o$ corresponding to the rubbing direction and it is parallel with incident p-polarized light. In the S_{in}/S_{out} polarization combination, the SHG intensity is minimum at the same ψ, when the fundamental beam of s-polarized light is perpendicular to the rubbing direction.

Figure 5.3 shows the contribution of each nonlinear susceptibility element to the theoretical SHG data in figure 5.2. Here we assumed $\chi^{(2)}_{zyy}$ and $\chi^{(2)}_{yzy}$ as zero which will be explained in eq. (5.16). Several elements of the nonlinear susceptibility have negative interference with each other during the numerical minimization of the summed squared deviations, and the fitting result was stabilized when I took the contribution from $\chi^{(2)}_{xzz}$, $\chi^{(2)}_{xxz}$, $\chi^{(2)}_{zxz}$, $\chi^{(2)}_{xyy}$, and $\chi^{(2)}_{yxy}$ elemements in one group. Table 5.1 shows the nonlinear susceptibility elements obtained by this fitting for the rubbed polyimide. The values of $\chi^{(2)}_{xzz}$, $\chi^{(2)}_{xxz}$, $\chi^{(2)}_{zxz}$, $\chi^{(2)}_{xyy}$, and $\chi^{(2)}_{yxy}$ elemements are not shown because they are not stable separately. The $\chi^{(2)}_{ijk}$ values are normalized so that $\chi^{(2)}_{zzz}$ becomes unity in the complex plane.

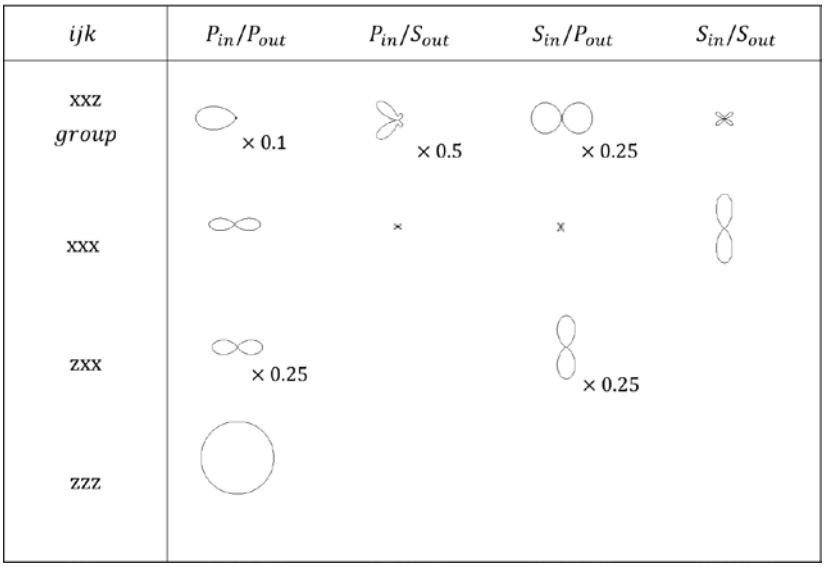

Fig. 5.3. SHG intensity contribution from each $\chi_{ijk}^{(2)}$ element decomposed in the theoretical patterns in Fig. 5.2. xxz group contains the contribution from xxz, xzz, zxz, xyy, and yxy components. The scales are common to all the patterns except indicated otherwise.

Table 5.1: Second order nonlinear susceptibility elements $\chi_{ijk}^{(2)}$ of the rubbed polyimide sample. The values of $\chi_{ijk}^{(2)}$ are normalized by that of $\chi_{zzz}^{(2)}$.

ijk	$\chi_{ijk}^{(2)}$
xxx	(0.09803 , 0.004661)
zxx	(0.4107 , -0.0240)
zzz	(1.0000 , 0.0000)
yyz	(0.0 , 0.0)
zyy	(0.0 , 0.0)
xxz	(--- , ---)
yyx	(--- , ---)
xyy	(--- , ---)
xzz	(--- , ---)
zxz	(--- , ---)

5.3 Molecular orientation of the rubbed polymer chain

In order to find the molecular orientational distribution of the rubbed polymer chain, I need to convert the information given by the macroscopic nonlinear susceptibility elements $\chi_{ijk}^{(2)}$ to a microscopic polymer chain polar angle. For this purpose, I assumed simply that polymer units have one dominant component $\beta_{\xi\xi\xi}^{(2)}$ along the axis ξ as shown in Fig. 5.4. This is an approximation adopted by other papers [4], although it is a crude assumption and should be revised in a more sophisticate analysis in the future.

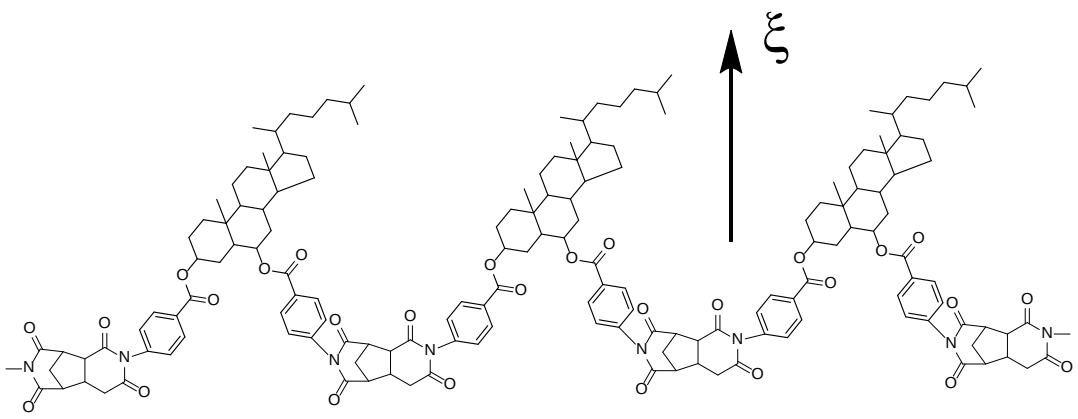

Fig. 5.4. Structure of polyimide with steroid side chain diamine A

The relation between the nonlinear susceptibility and molecular nonlinear polarizability is given as [4],

$$\chi_{ijk}^{(2)} = N_s < (\hat{i}.\hat{\xi})(\hat{j}.\hat{\xi})(\hat{k}.\hat{\xi} > \beta_{\xi\xi\xi}^{(2)} \qquad (5.7)$$

Here N_s is the molecular density of the surface, i, j and k denote the sample coordinate x, y, or z, and the bracket sign indicates the average over molecular orientational distribution function. The individual components of the nonlinear susceptibility $\chi^{(2)}_{ijk}$ give the information about the orientation and arrangement of the molecules of the rubbed polyimide layer. Relation of nonvanishing elements $\chi^{(2)}_{ijk}$ and a hyperpolarizability $\beta^{(2)}_{\xi\xi\xi}$ directed at the polar angle (θ, Φ) are [5],

$$\chi^{(2)}_{zzz} = N_s < cos^3\theta > \beta^{(2)}_{\xi\xi\xi} \quad (5.8)$$

$$\chi^{(2)}_{xxx} = N_s < sin^3\theta\, cos^3\Phi > \beta^{(2)}_{\xi\xi\xi} \quad (5.9)$$

$$\chi^{(2)}_{zyy} = \chi^{(2)}_{yzy} = \chi^{(2)}_{yyz} = N_s < (cos\theta - cos^3\theta)(1 - cos^2\Phi) > \beta^{(2)}_{\xi\xi\xi} \quad (5.10)$$

$$\chi^{(2)}_{zxx} = \chi^{(2)}_{xzx} = \chi^{(2)}_{xxz} = N_s < (cos\theta - cos^3\theta)(cos^2\Phi) > \beta^{(2)}_{\xi\xi\xi} \quad (5.11)$$

$$\chi^{(2)}_{zxz} = \chi^{(2)}_{zzx} = \chi^{(2)}_{xzz} = N_s < (sin\theta - sin^3\theta)(cos\Phi) > \beta^{(2)}_{\xi\xi\xi} \quad (5.12)$$

$$\chi^{(2)}_{xyy} = \chi^{(2)}_{yxy} = \chi^{(2)}_{yyx} = N_s < (sin^3\theta)(cos\Phi - cos^3\Phi) > \beta^{(2)}_{\xi\xi\xi} \quad (5.13)$$

If we assume that the polymer molecules are tilted in x direction, Φ is zero. If we assume that the polar angle θ is distributed around θ_{ave} then eqs. (5.8) to (5.13) are approximated as,

$$\chi^{(2)}_{zzz} \approx N_s cos^3\theta_{ave} \beta^{(2)}_{\xi\xi\xi} \quad (5.14)$$

$$\chi_{xxx}^{(2)} \approx \mathrm{N_s} sin^3\theta_{ave}\, \beta_{\xi\xi\xi}^{(2)} \tag{5.15}$$

$$\chi_{zyy}^{(2)} = \chi_{yzy}^{(2)} = \chi_{yyz}^{(2)} \approx 0 \tag{5.16}$$

$$\chi_{zxx}^{(2)} = \chi_{xzx}^{(2)} = \chi_{xxz}^{(2)} \approx \mathrm{N_s} sin^2\theta_{ave} cos\theta_{ave} \beta_{\xi\xi\xi}^{(2)} \tag{5.17}$$

$$\chi_{zxz}^{(2)} = \chi_{zzx}^{(2)} = \chi_{xzz}^{(2)} \approx \mathrm{N_s} sin\theta_{ave} cos^2\theta_{ave} \beta_{\xi\xi\xi}^{(2)} \tag{5.18}$$

$$\chi_{xyy}^{(2)} = \chi_{yxy}^{(2)} = \chi_{yyx}^{(2)} \approx 0 \tag{5.19}$$

From eqns. (5.14) and (5.15) I obtain,

$$tan^3\theta_{ave} = \frac{\chi_{xxx}^{(2)}}{\chi_{zzz}^{(2)}} \tag{5.20}$$

from eqns. (5.15) and (5.17) I have,

$$tan\theta_{ave} = \frac{\chi_{xxx}^{(2)}}{\chi_{zxx}^{(2)}} \tag{5.21}$$

and from eqns. (5.15) and (5.18) I have,

$$tan^2\theta_{ave} = \frac{\chi_{xxx}^{(2)}}{\chi_{zxz}^{(2)}} \tag{5.22}$$

Taking the absolute values of $\chi^{(2)}_{xxx}$, $\chi^{(2)}_{zzz}$, $\chi^{(2)}_{zxx}$ *and* $\chi^{(2)}_{zxz}$, the tilt angle of polymer side chain towards the rubbing direction can be calculated the by using equation (5.20) to (5.22). The values of $\chi^{(2)}_{xxx}$, and $\chi^{(2)}_{zxx}$ were calculated from the fitting results of the SHG patterns. The tilt angle of the polymer chains diamine can be determined. It is θ_{ave}= 15.7^o $\pm$ 1.8^0 from equation (5.21). The error was calculated from the data of four independent measurements in the same condition. This means that the polymer chain tilted by about 16^o from the surface normal at $\Phi = 0°$. This result is illustrated schematically in Fig. 5.5. Here I disregarded the small phase shift between the $\chi^{(2)}$ elements in Table 5.1 and simply took the ratio of their absolute value as an approximation in evaluating θ_{ave} from eqn. (5.21). I did not use eq. (5.20) because $\chi^{(2)}_{zzz}$ may have a bigger error than $\chi^{(2)}_{xxx}$, and $\chi^{(2)}_{zxx}$. Namely, since Fig. 5.3 shows that the SHG intensity patterns have contributions from many $\chi^{(2)}_{ijk}$ elements, the fitting can have more ambiguity of the values of the susceptibility elements. On the other hand, $\chi^{(2)}_{xxx}$ is the only component having contribution at 90^o for Sin/Sout configuration, and $\chi^{(2)}_{zxx}$ at 90^o for Sin/Pout configuration, so they are considered quite reliable.

The real chain of polyimide takes a zigzag structure as shown in Fig. 5.5. Before the rubbing treatment, the molecular distribution is polar with respect to the surface normal and the chains are oriented in random directions. The side chains are exposed on the film surface because of their hydrophobicity. By the rubbing treatment, the side chains are thought to be pulled on the surface by the nylon cloth and the main zigzag chains lying perpendicular to the rubbing direction are pulled and in average tilt in the rubbing direction as schematically shown in Fig. 5.5. The flexibility of the zigzag chains permits the change of the structure by the rubbing treatment.

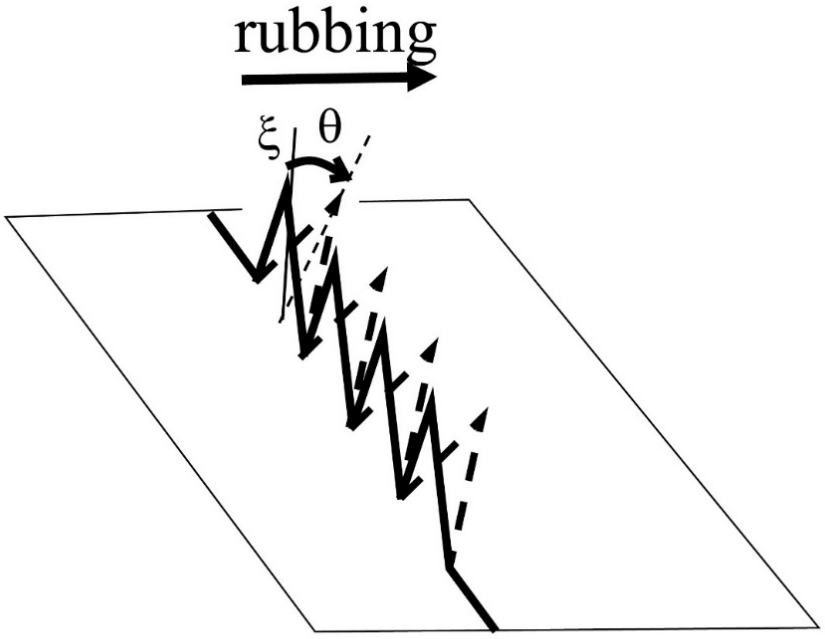

Fig. 5.5. Schematic model of the rubbing effect of the polyimide with steroid side chain

5.4 Significance of the evaluation of the molecular orientation of the rubbed polymer chain in the complex $\chi^{(2)}$

Second order nonlinear optical method, namely, second harmonic generation (SHG) has been received attention as excellent technique for studying surfaces and interface, because of its surface specificity and versatility [6-7]. The phase of the second order nonlinear of surface molecules can provide useful information about their directionality of the molecular orientation. Consider the following relation for an oriented layer of SHG active molecules on a substrate [8].

$$\chi^{(2)} = \mathrm{N} < \beta^{(2)} > \qquad (5.23)$$

where N is the molecules per unit area. A comparison of the phase between macroscopic nonlinear susceptibility $\chi^{(2)}$ and microscopic nonlinear polarizability, $\beta^{(2)}$ will give the information on the molecular orientation (or directionality) with respect to the surface normal. As with complex number, there is a phase associated with the imaginary part (resonant contribution to the second order susceptibility,$\chi_R^{(2)}$). This differ from the real part of $\chi^{(2)}$ (non-resonant contribution, $\chi_{NR}^{(2)}$). Then, one or more electronic resonances each with their individual phase can interfere with the non-resonant second order susceptibility in second harmonic generation.

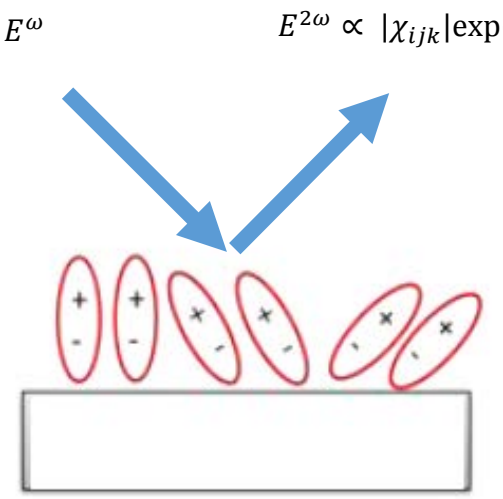

Fig. 5.6 Dipole model

Previously, in most reports, the amplitude of second order nonlinear susceptibility components, $|\chi_{ijk}^{(2)}|$ were considered as real values for the determination of the molecular orientation of rubbed polyimide [9-10]. However, $\chi_{ijk}^{(2)}$ has not only a real part but also imaginary part ($\mathrm{Im}\chi_{ijk}^{(2)}$) because χ_{ijk} is a complex number, and it is

expressed as

$$\chi_{ijk} = |\chi_{ijk}|\exp(i\varphi_{ijk}) \quad (5.24)$$

where φ_{ijk} is the phase of the χ component, which appears as a phase shift between SHG field and fundamental field. Therefore, χ_{ijk} has no longer a real number only but with the imaginary part due to the phase shift. The imaginary terms,($\mathrm{Im}\chi^{(2)}_{ijk}$) are associated with the fluctuation dielectric property of material. It follows dissipation-fluctuation theorem [11]. The complex dielectric permittivity is given by $\varepsilon(\omega) = \varepsilon'(\omega) - i\varepsilon''(\omega)$, where ε' is the relative permittivity (static dielectric contribution) and ε'' is the energy loss in dielectric medium. The complex susceptibility $\chi(\omega)$ is associated with complex permittivity $\varepsilon(\omega)$. The behavior of the imaginary part of complex dielectric permittivity is due to the fact from compositional fluctuation (may originate from the preparation process and statistical fluctuation) and structural defect [12]. This fluctuation field will create inhomogeneous molecular orientation in the surface [13]. Therefore, in reality, it is very much necessary to consider the $\chi^{(2)}$ component in the complex plane. In this regard, I analyzed the SHG patterns with the nonlinear susceptibility components in complex plane and also evaluated the molecular orientation i.e. tilt angle of the polymer side chain, which is the first report in my thesis under consideration of complex $\chi^{(2)}$. However, it is difficult to deduce some information from this imaginary part, and it should be a research topic in the future.

References:

[1] L.U. Rong and W. H. Fei, Chin. Phys. Lett. 20, 1269 (2003)

[2] B. Jerome and Y. R. Shen, Phys. Rev. E, 48, 4556 (1993)

[3] Y. R. Shen, Annu. Rev. Phys. Chem. 40 32 (1989)

[4] K. Shirota, K. Ishikawa, H. Takezoe, A. Fukuda and T. Shibashi, Jpn. J. Appl. Phys. 34, L316 (1995)

[5] W. Chen, M. B. Feller and Y. R. Shen, Phys. Rev. Lett., 63(24) 2665 (1989)

[6] H. Sano, J. Saito, J. Ikeda and G. Mizutani, J. Appl. Phys. 100, 043710 (2006)

[7] A. B. El Basaty, Y. Miyauchi, G. Mizutani, T. Matsushima and H. Murata; Appl. Phys. Lett. 97**,** 193302 (2010)

[8] R. Stolle, G. Marowsky, E. Schwarzberg and G. Berkovic, Appl. Phys. B. 63 , 491 (1996)

[9] J. J. Ge, C. Y. Li, G. Xue, I. K. Mann, D. Zhang, S. Y. Wang, F. W. Harris, S. Z. D. Cheng, S. C. Hong, X. Zhuang, and Y. R. Shen, J. Am. Chem. Soc. 123, 5768, (2001)

[10] J. Y. Huang, J. S. Li, Y. S. Juang and S. H. Chen, Jpn. J. Appl. Phys. 34, Pt. 1, No. 6A, 3163 (1995)

[11] R. Kubo, Rep. Prog. Phys. 29, 255 (1996)

[12] V.K. Komar, V.P. Migal, D.P. Nalivaiko, O.N. Chugai, Inorg. Mater. 37 449 (2001)

[13] S. Z. Ngah Demon, Y. Miyauchi, G. Mizutani, T. Matsushima and H. Murata, Appl. Surf. Sci. 311, 715 (2014)

Chapter 6

General Conclusion

The different type of liquid crystal displays (LCDs) dominate the electronics market for flat panel displays. The advantages of these devices are low weight, thin planner construction, low operating voltages and power consumption, and high contrast, and large viewing angles. The market for the flat panel displays is expanding rapidly with the popularity of digital watches, calculators, notebook computers, hand-held computer games and toys, mobile telephones, digital cameras, etc. A novel alignment method, namely, the rubbing method, turns to align the LCs layer on the surface. The alignment mechanism of liquid crystals (LCs) is not only important in scientific interest but also of technological importance for display device performance. Among various polymers, polyimide (PI) is considered the most effective polymeric material, which is used as the alignment film in LCDs because of its high thermal stability, high transition temperature (T_g), and also high orientation stability. In other important terms, the generation of the pretilt angle is very necessary for the ability of LCDs performance such as high contrast, fast response time, and wider viewing angle. From that points of view, a novel polyimide alignment films require synthesis for generating the larger pretilt angle, say, from 3 to 90^o .

Optical second harmonic generation (SHG) has been largely used for studying the surface and interface phenomena as an excellent technique. But, there are very limited research works done on polyimide by using SHG method. I surveyed the number of research study on polyimide by SHG. The number of SHG works of

polyimide is not big enough. In this regard, research work on polyimide alignment thin film by optical SHG needs a development for improving the performances of LCDs device. Therefore, I would like to contribute to developing the research work on polyimide alignment thin film by optical SHG.

In this study, in collaboration with JSR Co. Ltd., a novel rubbed and unrubbed PI with steroidal structure side chain diamine A (PAA-1) were synthesized. The PI film was rubbed by a rubbing machine using nylon cloth. The rotational speed of the roller and the translational speed were 400 rpm and 30 mm/sec, respectively. The thickness of the PI film was 100 nm. So far as I know, there has been no SHG measurement of polyimide polymers with steroidal structures. This study is the first report to find the molecular orientation of side chain of diamine A (PAA-1) by applying SHG measurement. In this regard, I observed the rotational and polarization dependence of SHG intensity from the both unrubbed and rubbed PI thin films with steroidal structure side chains diamine A. The SHG patterns from the unrubbed PI films is isotropic. In this case, the molecular distribution is polar with respect to the surface normal and the chains are oriented in random directions. On the other hand, the characteristic anisotropic patterns of the rubbed PI thin film samples are observed due to the rubbing.

In order to find the molecular orientation of the rubbed polymer chains, I assumed that polymer units have one dominant component $\beta^{(2)}_{\xi\xi\xi}$ along the molecular axis ξ. The individual components of the nonlinear susceptibility $\chi^{(2)}_{ijk}$ of PI film surface can be calculated via $\beta^{(2)}_{\xi\xi\xi}$ and give the information about the orientation and arrangement of the molecules of the rubbed polyimide layer. Previously, in most reports, the

amplitude of second order nonlinear susceptibility components, $|\chi_{ijk}^{(2)}|$ were considered as real values for the determination of the molecular orientation of rubbed polyimide. However, $\chi_{ijk}^{(2)}$ has not only a real part but also imaginary part ($\mathrm{Im}\chi_{\mathrm{ijk}}^{(2)}$) because χ_{ijk} is a complex number, and it is given by $\chi_{\mathrm{ijk}} = |\chi_{ijk}|\exp(i\varphi_{ijk})$, where φ_{ijk} is the phase of the χ component, which appears as a phase shift between SHG field and fundamental field. Therefore, χ_{ijk} has no longer a real number only but with the imaginary part due to the phase shift. The imaginary terms, ($\mathrm{Im}\chi_{\mathrm{ijk}}^{(2)}$) associated with the fluctuation dielectric property of material. This fluctuation field will create inhomogeneous molecular orientation in the surface. Therefore, in reality, it is necessary to consider the χ component in the complex plane. In this regard, I analyzed the SHG patterns with the second order nonlinear susceptibility components $\chi_{ijk}^{(2)}$ in complex plane, which is the first report in my thesis. I took the magnitude of the absolute value from $\chi_{xxx}^{(2)}$ and $\chi_{zxx}^{(2)}$ components, and finally I determined the average tilt angle of the polymer main chain toward the rubbing direction as θ_{ave}= $15.7^{o} \pm 1.8^{0}$. The strong point in this analysis is that I considered the values of $\chi_{\mathrm{ijk}}^{(2)}$ elements in the complex plane.

Before the rubbing treatment, the polymer chains are oriented randomly with respect to the surface normal. After the rubbing treatment, the side chains are thought to be pulled on the surface. The main zigzag chains lying perpendicular to the rubbing direction are pulled and in average tilt in the rubbing direction. This happened due to the flexibility of the zigzag chains, which permits the change of the structure by the rubbing treatment.

This study established the first step to the development and application of polyimide films with steroidal side chains using SHG spectroscopy in the liquid crystal device technology.

Appendix I:
Synopsis of Minor Research

In cellular and molecular biology, cell culture is a significant method, which provided a model systems for studying of the physiology and biochemistry of cells. HEK293 cells and HeLa cells were cultured through Dulbecco's Modified Eagle Medium (DMEM) containing 10% fetal bovine serum (FBS) in a standard CO_2 incubator, where CO_2 incubators allow to better control of culture conditions. Cell passages were performed using standard trypsin/EDTA method. Cell density was estimated by using an erythrocytometer (Thoma-type). Cell suspension at the concentration of 10^7 cells / ml was then prepared. The number of cells were counted by a cell counter in this process. At the last stage of cell culture, the reporter gene plasmid, EGFP/pcs4+, was added to the suspension at the concentration of 0.1 μg/μl. On the other hand, a well established technique , electroporation or electropermeabilization was used in which the application of an external electric field pulse leads to an increase in the permeability of cellular membranes. Home-made electrodes were used in this measurement, where the carbon rods with diameter of 2mm was vertically positioned in this instrument. The voltage waveforms were generated by using AWG-50 (Elmos), an arbitral waveform generator with an aid of supplied software. To find optimal condition of electroporation, FPs (first pulse) and SPs (second pulse) were attenuated by a certain factor and different combinations of these pulses were applied and evaluated GFP expression. In this regard,EGFP was investigate in the nucleus and in the cytoplasm of HeLa and HEK293 cells by optical microscope. Transmission image and fluorescence image were taken at different combinations of these pulses, (FPs+SPs) for both type of cells. Finally, the loading efficiency of all cell were found by the fluorescence image in this study.

Appendix II:
Monochromator Sensitivity (1F pico second laser lab)

Due to calibration our experimental data of wavelength 532 nm, I checked the monochromator sensitivity in terms of SHG intensity and both horizontal (p-polarized) and verical(s-polarized) output polarization. For this purpose, I kept the experimental setup according to the following figure:

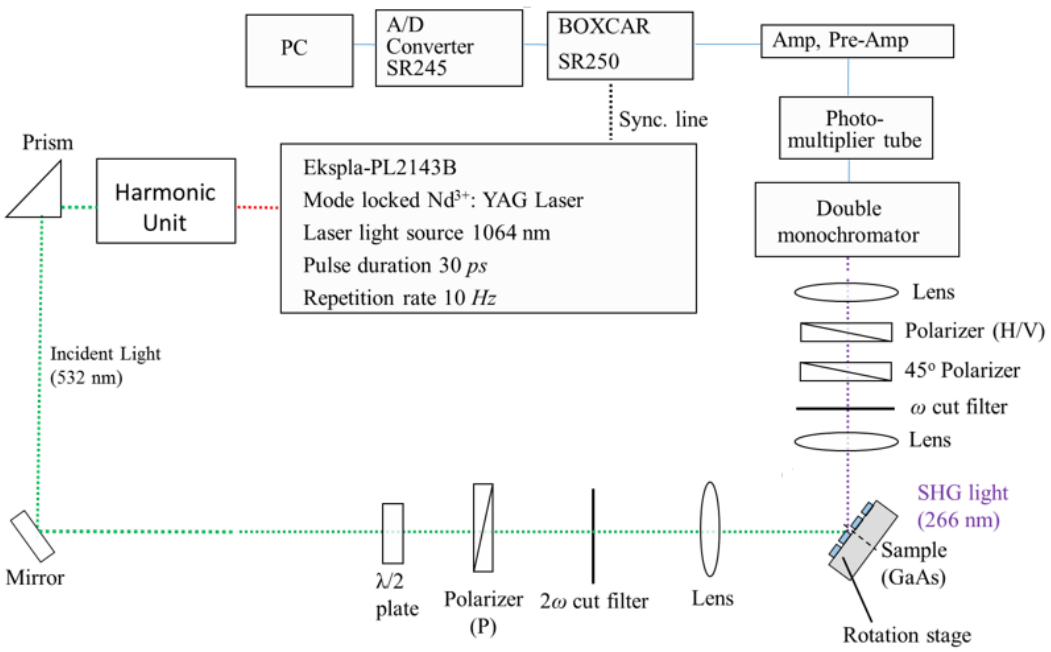

Figure 1: Optical setup for monochromator sensitivity check

Figure 1. shows that the incident light of wavelenght 532 nm was irradiated on the GaAs (100) sample. The reflected light was passesd through lens, ω-cut filter, 45° polarizer, horizontal or vertical polarizer to obtain the SHG signal due to compare the SHG intensity difference for horizontal and vertical output polarization in order to check the sensitivity of monochromator.

Table 1: Monochromator Sensitivity

Symbols: P= Horizontal polarization: 0, S= Vertical polarization: 1

Polarization	Intensity (a.u.)	Average Intensity (a.u.)	Ratio: S/P	Average (S/P)
0	25.424			
0	27.514	26.47		
1	28.617		1.07	
1	28.176	28.34		
0	20.449			
0	21.949	21.20		
1	22.726		1.19	
1	27.977	25.35		
0	21.434			
0	20.291	20.86		
1	28.213		1.23	
1	23.453	25.82		
0	18.681			1.17
0	16.02	17.35		
1	20.86		1.26	
1	23.047	21.95		
0	18.593			
0	18.104	18.34		
1	20.976		1.08	
1	18.648	19.812		
0	20.938			
0	17.779	19.35		
1	21.73		1.19	
1	24.583	23.156		

Appendix III:
List of publication/conference proceedings

Journal:

1. Muhammad Samir Ullah, Shohei Asai, Yousuke Inomata, Khuat Thi Thu Hien, Goro Mizutani, Yoshitaka Murakami and Takashi Okada, “Optical second harmonic generation study of a rubbed polyimide film containing steroidal structure side chains ” e-J. Surf. Sci. Nanotech. Vol. 15 (2017) 7-12.

Conference Proceedings:

1. Muhammad Samir Ullah, Siti Zulaikha Ngah Demon, Kazuki Matsumoto, Yoshihiro Miyauchi, Khuat Thi Thu Hien, Goro Mizutani and Harvey Rutt ; “Nonlinear optical interferometry study at the interface of organic thin films with indium tin oxide”. The 26th Symposium of Association for Condensed Matter Photophysics, Japan, 11-12 December, 2015.

2. Muhammad Samir Ullah, Siti Zulaikha Ngah Demon, Kazuki Matsumoto, Khuat Thi Thu Hien, Goro Mizutani and Harvey Rutt ; “New Method for Analyzing the Second Harmonic Generation Phase from the Interface between Indium Tin Oxide and Organic Layer”. 10th International Symposium on Atomic Level Characterizations for New Materials and Devices ’15, 25-30 October, 2015, in Matsue, Shimane, Japan

3. Kazuki Matsumoto, Siti Zulaikha Ngah Demon, Muhammad Samir Ullah, Goro Mizutani, Khuat Thi Thu Hien; “Detection of the phase shift from dipole layer of the organic semiconductor by Second Harmonic Generation”, The 25th Symposium of Association for Condensed Matter Photophysics, Japan, 12-13 December, 2014.

4. Shohei Asai, Muhammad Samir Ullah, Yousuke Inomata, Khuat Thi Thu Hien, Goro Mizutani, Yoshitaka Murakami and Takashi Okada, **“**Surface anisotropy characteristics of polyimide alignment film by nonlinear optical method” The 27th Symposium of Association for Condensed Matter Photophysics, Japan, 2-3 December, 2016.

Attended Conferences/Symposium/Workshop

1. **Muhammad Samir Ullah**, Siti Zulaikha Ngah Demon, Kazuki Matsumoto, Khuat Thi Thu Hien, Goro Mizutani, Heisuke Sakai, Toshinori Matsushima and Hideyuki Murata; “Observation of Optical Second Harmonic Generation Interference Pattern for ITO/MTDATA system”. The 2nd JAIST Poster Challenge, JAIST Festival, Japan, 11 October, 2014.

2. **Muhammad Samir Ullah**, Siti Zulaikha Ngah Demon, Kazuki Matsumoto, Khuat Thi Thu Hien, Goro Mizutani, Heisuke Sakai, Toshinori Matsushima and Hideyuki Murata; “Optical Second Harmonic Investigation of the ITO/MTDATA/Al OLED Device”, The 7th International Symposium on Surface Science (ISSS-7), Matsui, Shimane, Japan, 2-6 November, 2014.

3. Kazuki Matsumoto, Siti Zulaikha Ngah Demon, **Muhammad Samir Ullah**, Goro Mizutani, Khuat Thi Thu Hien; “Detection of the Phase Shift from Dipole Layer of the Organic Semiconductor by Second Harmonic Genration”, The 25th Symposium of Association for Condensed Matter Photophysics, Japan, 12-13 December, 2014.

4**. Muhammad Samir Ullah,** Siti Zulaikha Ngah Demon, Kazuki Matsumoto, Khuat Thi Thu Hien, Goro Mizutani and Harvey Rutt ; “Study of Optical Second Harmonic Interference Pattern at Interface between Iron Phthalocyanine Layer and Indium Tin Oxide” JPS meeting-2015, 16-19 September, 2015 at Kansai University, Japan.

5. **Muhammad Samir Ullah,** Siti Zulaikha Ngah Demon, Kazuki Matsumoto, Khuat Thi Thu Hien, Goro Mizutani and Harvey Rutt ; “New Method for Analyzing the Second Harmonic Generation Phase from the Interface between Indium Tin Oxide and Organic Layer”. 10th International Symposium on Atomic Level Characterizations for New Materials and Devices ’15, 25-30 October, 2015, in Matsue, Shimane, Japan

6. **Muhammad Samir Ullah**, Siti Zulaikha Ngah Demon, Kazuki Matsumoto, Khuat Thi Thu Hien, Goro Mizutani and Harvey Rutt;“ Phase of the Second Order Nonlinear Susceptibility at the Interface of Indium Tin Oxide/Organic Semiconductor”. JAIST Symposium on Advanced Science & Technology 2015 (JAIST SAST 2015), 11-12 November, 2015, JAIST, Japan.

7. **Muhammad Samir Ullah**, Siti Zulaikha Ngah Demon, Kazuki Matsumoto, Yoshihiro Miyauchi, Khuat Thi Thu Hien, Goro Mizutani and Harvey Rutt ; “Nonlinear optical interferometry study at the interface of organic thin films with indium tin oxide”. The 26th Symposium of Association for Condensed Matter Photophysics, Japan, 11-12 December, 2015.

8. **Muhammad Samir Ullah**, Siti Zulaikha Ngah Demon, Kazuki Matsumoto, Yoshihiro Miyauchi, Khuat Thi Thu Hien, Goro Mizutani and Harvey Rutt ;“Measurement of the Absolute Phase at the Interface of Organic Semiconductor by Second Harmonic Interference Technique”. II-Sc-JAIST Joint Workshop on Functional Inorganic and Organic Materials, Japan, 7 March, 2016.

9**. Muhammad Samir Ullah**, Siti Zulaikha Ngah Demon, Kazuki Matsumoto, Yoshihiro Miyauchi, Khuat Thi Thu Hien, Goro Mizutani and Harvey Rutt ; “Investigation of the Phase Shift at the Interface of the Functional Organic Materials by Nonlinear Optical Method”. JPS meeting-2016, 13-16 September, 2016 at Kanazawa University, Japan.

10. **Muhammad Samir Ullah**, Siti Zulaikha Ngah Demon, Kazuki Matsumoto, Yoshihiro Miyauchi, Khuat Thi Thu Hien, Goro Mizutani and Harvey Rutt ; “Theoretical Approach of the Nonlinear Second Harmonic Interferometry Technique: Case Study for Organic Semiconductor Interface”. Organic and Inorganic Electronics Symposium: O & I Symposium, 15-16 July, 2016

11. Shohei Asai, **Muhammad Samir Ullah**, Yousuke Inomata, Khuat Thi Thu Hien, Goro Mizutani, Yoshitaka Murakami and Takashi Okada, **“**Surface anisotropy characteristics of polyimide alignment film by nonlinear optical method” The 27th Symposium of Association for Condensed Matter Photophysics, Japan, 2-3 December, 2016.

12. Yousuke Inomata, **Muhammad Samir Ullah**, Shohei Asai, Khuat Thi Thu Hien, Goro Mizutani, Yoshitaka Murakami and Takashi Okada, **“**Study of the structure of constituent molecules of a liquid crystal panel substrate by SHG spectroscopy” JPS meeting-2017, 17-20 March, 2017 at Osaka, Japan.

13. **Muhammad Samir Ullah**, Shohei Asai, Yousuke Inomata, Khuat Thi Thu Hien, Goro Mizutani, Yoshitaka Murakami and Takashi Okada, Observation of rubbing induced molecular orientation of polyimide containing a flexible structure by second harmonic generation, JAIST-India Symposium on Materials Science 2017, 6-7 March, 2017, JAIST, Japan.

Award:

1) Best Poster Award in JAIST Symposium on Advanced Science & Technology 2015 (JAIST SAST 2015), 11-12 November, 2015, JAIST, Japan.

2) JAIST President Award 2016, 02 March, 2017, JAIST, Japan.